THESIS

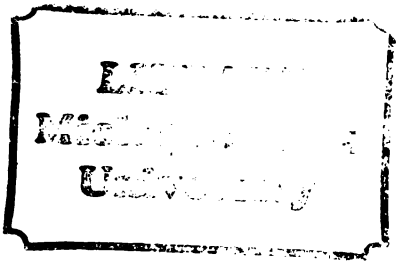

This is to certify that the

dissertation entitled

INFLUENCE OF HYDROSTATIC PRESSURE
ON GAS BALANCE AND LACUNAR STRUCTURE
IN *MYRIOPHYLLUM SPICATUM* L.

presented by

Frederick Carroll Payne

has been accepted towards fulfillment
of the requirements for

Ph.D. degree in Limnology

C. D. McNabb
Major professor

Date May 12, 1982

MSU is an Affirmative Action/Equal Opportunity Institution

O-12771

MSU
LIBRARIES

RETURNING MATERIALS:
Place in book drop to remove this checkout from your record. FINES will be charged if book is returned after the date stamped below.

INFLUENCE OF HYDROSTATIC PRESSURE ON GAS BALANCE AND LACUNAR STRUCTURE IN *MYRIOPHYLLUM SPICATUM* L.

By

Frederick Carroll Payne

G 11786

A DISSERTATION

Submitted to
Michigan State University
in partial fulfillment of the requirements
for the degree of

DOCTOR OF PHILOSOPHY

Department of Fisheries and Wildlife

1982

ABSTRACT

INFLUENCE OF HYDROSTATIC PRESSURE
ON GAS BALANCE AND LACUNAR STRUCTURE
IN *MYRIOPHYLLUM SPICATUM* L.

By

Frederick Carroll Payne

In very clear lakes, non-lacunate hydrophytes grow to great depths; their lower limits appear to be determined by light quantity or quality. Lacunate hydrophytes are restricted to much shallower regions of clear lakes. Hydrostatic pressure may limit distribution of the lacunate hydrophytes. A general model for gas balance in lacunae, cell sap and surrounding water for submersed vascular hydrophytes showed that hydrostatic pressure restricts the development of lacunar spaces as long as lacunar gas pressures reflect hydrostatic pressure.

An experimental system was developed to allow independent control of hydrostatic pressure and light intensity, with gas levels maintained at atmospheric partial pressures. Results of experiments on net oxygen efflux and lacunar oxygen storage confirmed the general gas balance model, but showed that hydrostatic pressure had no influence on shoots of *Myriophyllum spicatum* L. The proposed mechanism for hydrostatic pressure limitation required that lacunar gas

pressures be determined by the prevailing hydrostatic pressure. This condition was not met by shoots of *Myriophyllum spicatum*.

Anatomical studies revealed a *lacunar arch system* in stems of *Myriophyllum spicatum* which was capable of expanding the lacunae against external forces on the strength of cell turgor pressure. Plants grown at 83 kPa hydrostatic pressure had normal anatomy. The lacunar arch system appeared strongest in young, apical shoots like those tested in the net oxygen efflux and lacunar storage experiments. Mature shoots collected from outdoor stock ponds had weaker lacunar arch structures suggesting greater susceptibility to external compression forces such as hydrostatic pressure. The lysigenous lacunae of *Myriophyllum spicatum* roots had no organized lacunar structure and therefore offer little resistance to external crushing forces.

This research failed to demonstrate a mechanism for hydrostatic pressure limitation of lacunate hydrophytes. It did suggest a mode of lacunar expansion not described in the literature. Exapnsion of the lacunar arch structure by cell turgor pressure may explain the lack of hydrostatic pressure effects on apical shoot sections. Weakening of the lacunar arch system in older stems, as well as weakness of the root lacunar system, remain as likely explanations for the hydrostatic pressure limitation of lacunate hydrophytes in lakes.

ACKNOWLEDGMENTS

My wife, Therese, is recognized by all as my principle source of support throughout my graduate programs. Her continuing love, encouragement and, no least of all, financial support made my accomplishment possible.

I sincerely thank Professor C.D. McNabb for his guidance and assistance during his time as my major professor.

My graduate guidance committee, Professors N.R. Kevern, P.G. Murphy and R.G. Wetzel, was invaluable in planning and discussing my research and reviewing this dissertation. Special thanks go to Professor Wetzel who provided me with the opportunity to study pressure effects on seagrasses; this experience fundamentally influenced my approach to macrophyte - pressure relationships.

The experiments described here were made possible through the assistance of fellow graduate student Jane L. Schuette. Jane's knowledge of histological technique and her professional laboratory presence cannot be overstated.

I also thank fellow graduate students Ted Batterson and Robert Glandon for many fruitful discussions which preceded my experimentation.

I would finally like to thank Professor D.L. King for his sincere and undying interest in my research program.

The research facility for this dissertation was supported, in part, by funding from Project No. 959 of the Michigan Agricultural Experiment Station.

TABLE OF CONTENTS

LIST OF TABLES

LIST OF FIGURES

FIGURE PAGE

INTRODUCTION

Evidence for physical limitation of vascular hydrophyte distributions has been established by several authors. Pond (1905), Pearsall (1920) and Wilson (1935,1937,1941) showed the dependence of species distributions in lakes upon the texture, composition and accretion rate of substrata. Several authors concluded that light levels caused zonations of species in submersed hydrophyte communities (e.g., Pearsall, 1920; Wilson, 1935,1937,1941; Spence and Chrystal, 1970a,b; Sheldon and Boylen, 1977; Stross, 1979). The observations of Payne (1977) suggested that light and temperature both may have limited submersed hydrophyte distributions in arctic and subarctic lakes. Hutchinson (1975) has described limitations of hydrophytes by light, substratum and hydrostatic pressure.

The predictive value of any of these observed relationships is enhanced by knowledge of the mechanisms of limitation. The actions of light and temperature, for example, are well known from studies on terrestrial as well as aquatic species (e.g., Bonner and Varner, 1976; Salisbury and Ross, 1978). Although Gessner (1952), Fehrling (1957) and Golubic (1963) reported that hydrostatic pressure may limit the depth distribution of vascular hydrophytes in lakes, no mechanisms

of limitation have been identified. Vidaver (1972) reported that hydrostatic pressures greater than 200 atm (20,260 kPa) altered many metabolic activities in plants. However, the metabolic changes induced by pressures below 1,000 kPa were not measurable. Vidaver, (*Ibid.*) suggested that plants sensitive to pressures of 100 to 200 kPa (cf. Gessner, 1952, Fehrling, 1957, and Golubic, 1963) must possess a pressure "transducer"; a mechanism yet undiscovered, which is specifically sensitive to hydrostatic pressure.

Dale and coworkers (Bodkin, *et al.*, 1980; Dale, 1981) found that hydrostatic pressure did not influence growth of *Hippuris vulgaris* L. or *Myriophyllum spicatum* L., in contrast to results from Gessner (1952) and Golubic (1963), respectively. No generalizations can be made from any of the earlier studies because the experimental growing conditions almost certainly influenced their results, as will be shown below. The objectives of this study were to identify and test potential mechanisms for the limitation of vascular hydrophyte growth by hydrostatic pressure.

Field studies suggest that the angiosperm hydrophytes are restricted by hydrostatic pressure to depths less than 10-12 m (Hutchinson, 1975). Observations by Golubic (1963), Spence (1967), Frantz and Cordone (1967) and Sheldon and Boylen (1977) showed that submersed angiosperms do not exceed the 12 m depth, even in the clearest lakes. Golubic (1963) specifically tied this limit to hydrostatic pressure in Lake Vrana, where the light compensation point for shoots of

Myriophyllum spicatum, determined over a 20 h incubation period, occurred at the 36 m depth. The species was found to grow only to 7.7 m in the lake, 0.21 times the 20 h light compensation point.

Hydrostatic pressure does not appear to influence the depth distribution of non-vascular hydrophytes. These plants appear to be depth-limited by light, reaching the 1% isophote which extends to depths as great as 100 m in very clear lakes (Hutchinson, 1975; Frantz and Cordone, 1967). Stross (1979) tied the depth limit in *Nitella flexilis* L. to the influence of spectral composition of light on germination of dissemules. Golubic (1963) found *Chara fragilis* (*C. globularis*, Thuil.) and *C. polyacantha* (?) reached roughly 0.63 times their respective 20 h light compensation depths.

The observation which may explain the disparate response to depth by the vascular and non-vascular hydrophytes is the presence of lacunar spaces in the tissues of vascular hydrophytes. The schizogenous lacunae of leaf and stem tissues are free gas spaces which develop during normal differentiation (Sculthorpe, 1967). Root and rhizome tissues are usually found to have lysigenous lacunae (Sculthorpe, *Ibid.*). Dale (1957) proposed that schizogenous lacunae are formed when excess gas pressures achieved by photosynthetic oxygen production force open small spaces in the meristem region. The lysigenous lacunae are thought to form by the degeneration of cells and subsequent replacement by gases (Sculthorpe, 1967).

Lacunae are generally held to function as conduits for oxygen supply to buried organs and as reservoirs for the storage of gases of photosynthetic or respiratory origin (Hutchinson, 1975; Sculthorpe, 1967). The lacunae seem to be essential for maintaining internal gas balances, particularly in light of the relatively slow diffusion of gases in water. *Podostemum ceratophyllum* Michx., a non-lacunate vascular hydrophyte, does not support buried organs and is found only in flowing waters, where plant tissues are continuously bathed in water with gas levels near atmospheric saturation. We are led to suspect that any factor which can disrupt the normal formation or function of these air spaces can act to restrict the growth of the lacunate vascular hydrophytes.

If Dale's (1957) proposed mechanism for the formation of schizogenous lacunae is correct, gas pressure in these spaces must exceed the total pressure forcing on the plants' exterior surfaces; the lacunar gas pressures should be directly related to depth. Considerations of gas solubility and diffusion lead to specific predictions which demonstrate that hydrostatic pressure can be expected to disrupt lacunar formation and the storage of gases.

Henry's Law defines the solution of gases:

$$P_A = K \cdot X_A \qquad \text{(EQN 1)}$$

The vapor pressure of a solute, P_A, is proportional to its mole fraction, X_A, in solution. The constant of

proportionality, K, is the Henry's Law constant. K must be specified for the solute/solvent system at the temperature of interest.

For oxygen in an aqueous medium, it is more convenient to write Henry's Law as:

$$P_{O_2} = K'_{O_2} \cdot [O_2]_{aq} \qquad \text{(EQN 1A)}$$

where K'_{O_2} is expressed as $kPa \cdot mg^{-1} \cdot l$, $[O_2]_{aq}$ is in $mgO_2 \cdot l^{-1}$, and P_{O_2} is expressed in kPa. Approximate values of K'_{O_2} can be calculated for temperatures ranging from 5 to 30 C:

$$K'_{O_2} = 1.397 + 0.0462 \cdot T \qquad \text{(EQN 2)}$$

We can use Henry's Law to determine the vapor pressure of a solute in the atmosphere overlying a solution, or to determine the equilibrium concentration of a gas in solution given its partial pressure in the atmosphere. Henry's Law shows that an isolated column of pure water will have a uniform distribution of any ideal gas in the atmosphere overlying the column of water. Since the quantities of gas in the earth's atmosphere are large, we can view the atmosphere as the ultimate source or sink for equilibrating any consumption or evolution of gases in an aquatic system. Regardless of depth, lake waters tend toward atmospheric gas partial pressures.

Because lacunate hydrophytes maintain internal air spaces, it is important to consider some applications of Henry's Law. In the absence of surface tension or

confinement effects, the total gas pressure at any depth, z, is the sum of atmospheric (P_{atm}) and hydrostatic (P_h) pressures:

$$P_{tot} = P_{atm} + P_h \qquad \text{(EQN 3)}$$

and,

$$P_h = 9.80 \cdot z \qquad \text{(EQN 4)}$$

where P_h is expressed in kPa and z is given in m. Normal atmospheric pressure is 101 kPa; 10 m of water produces an additional 98 kPa hydrostatic pressure. The total gas pressure inside a gas space at the 10 m depth will be 199 kPa. If the gases dissolved in the water column are in equilibrium with the overlying atmosphere, Henry's Law points out that the water surrounding any gas space at the 10 m depth is undersaturated with respect to a 199 kPa air-water interface. Gases will exit the space; a gas space at depth can be maintained only in conjunction with some source of gas. The rate of supply from the source must equal the rate of solution into the surrounding medium to maintain steady-state gas space volume.

Dale (1957) suggested that oxygen evolved by photosynthetic hydrolysis of water is the principle source of gas for lacunar inflation. Carbon dioxide and methane may also be present at levels which exceed atmospheric saturation, but the partial pressures do not approach those of oxygen (Hartman and Brown, 1967). The minimum partial pressure of oxygen can be determined for a gas space at any depth:

$$P_{O_2} = P_{tot} - (P_{N_2} + P_{CO_2} + P_{CH_4} + P_{Ar} + \ldots) \quad \text{(EQN 5)}$$

where the sum of gases other than oxygen is approximately 80.1 kPa.

When a submerged gas space is at stable volume, the concentration of gases in the liquid phase surrounding the space are determined by Henry's Law. The dissolved oxygen concentration in the solution surrounding a gas space held open by excess oxygen pressure can be calculated from Equations 1A and 5. At 20 C, equilibrium oxygen concentrations outside a submerged gas space increase linearly from 9.1 $mgO_2 \cdot l^{-1}$ at 0 kPa hydrostatic pressure (at the water surface) to 52.4 $mgO_2 \cdot l^{-1}$ at 98 kPa hydrostatic pressure (10 m depth).

An oxygen gradient will be established in the water surrounding any gas space with oxygen partial pressures above normal atmospheric levels (e.g., in excess of 21.1 kPa O_2). For submersed vascular hydrophytes, the production of oxygen is concentrated in epidermal and mesophyll cells (cf. Grace and Wetzel, 1976, for *Myriophyllum spicatum*) which lie between the lacunae and the surrounding water. There are two gradients of oxygen diffusion from these source cells: one inward to the lacunar gas space and a second outward through the boundary region of still water surrounding the plant surface. The water outside the boundary region in the photic zone of lakes tends to be near atmospheric equilibrium due to bulk mixing processes (cf. Hutchinson, 1957).

The flux of oxygen through the gradients is defined

by Fick's First Law (Crank, 1956):

$$\text{FLUX} = \frac{\Delta \text{ CONCENTRATION} \cdot \text{SURFACE AREA}}{\text{RESISTANCE}} \qquad \text{(EQN 6)}$$

where Δ CONCENTRATION is the change in oxygen concentration from the highest to lowest concentrations in the gradient; SURFACE AREA is the surface area of the plant section from which the oxygen diffuses; RESISTANCE is the resistance to oxygen diffusion, a function of the diffusion coefficient for oxygen in water (for the outward gradient) or air (for the inward gradient), the shape of the diffusing body (e.g., planar, cylindrical or spherical), and the thickness of the still air or water region adjacent to the diffusing surface (boundary thickness).

For any plant section, the surface area and diffusion coefficient for oxygen can be considered as constant for both gradients. A specification of any two remaining variables (flux, boundary thickness or Δ concentration) determines the third. At steady state, the sum of oxygen fluxes through the inward and outward gradients equals the net photosynthetic rate. The rate of oxygen diffusion in the lacunar gas is 4 orders of magnitude faster than in water; thus the oxygen concentration in the lacunar gas will be relatively homogeneous. If the rate of oxygen consumption from the lacunar space is slow relative to the net photosynthetic rate, the lacunae act as dead space for gas accumulation. Under this condition, the concentration of oxygen at a plant's exterior

determines the partial pressure of oxygen in the lacunar space. It can be seen from Equation 6 that the concentration of oxygen at a plant's exterior surface is a function of the boundary layer thickness for any specified photosynthetic rate. Also, an increase in net photosynthesis increases the concentration at a plant's exterior surface under any specified boundary layer thickness.

Resistance to oxygen movement through the outward gradient can be viewed as *back-pressure* against which oxygen levels in the epidermis and mesophyll, and therefore also the lacunae, can build. Figure 1 provides a graphical representation of this viewpoint. In this diffusive gas equilibrium model, interplay between net photosynthetic rate and boundary layer thickness for the external oxygen gradient controls the partial pressure of oxygen in lacunar spaces. If oxygen partial pressures in lacunar spaces reflect hydrostatic pressures exerted on a plant's exterior, an increase in depth requires an increased oxygen concentration at the plant surface to hold back lacunar oxygen. Previous studies show that lacunar oxygen partial pressures probably cannot meet the demand of external hydrostatic pressures at depths greater than 1 or 2 m.

In studies reported by Hartman and Brown (1967), oxygen in lacunae of *Elodea canadensis* Michx. never exceeded 28% of the volume of gases present; nitrogen levels fluctuated between 75 and 85%. If lacunar volumes in these plants did not expand during the photosynthetic period, the highest

Figure 1. The diffusion-controlled gas equilibrium model for partitioning of oxygen in lacunar spaces, cell sap, and boundary water for lacunate hydrophytes. AMB indicates oxygen activity in water outside the boundary region; this is the atmospheric equilibrium level. Four conditions are represented: A. darkness; B. early morning; C. mid-day with minimum circulation of water surrounding the plant; D. mid-day with high circulation of surrounding water.

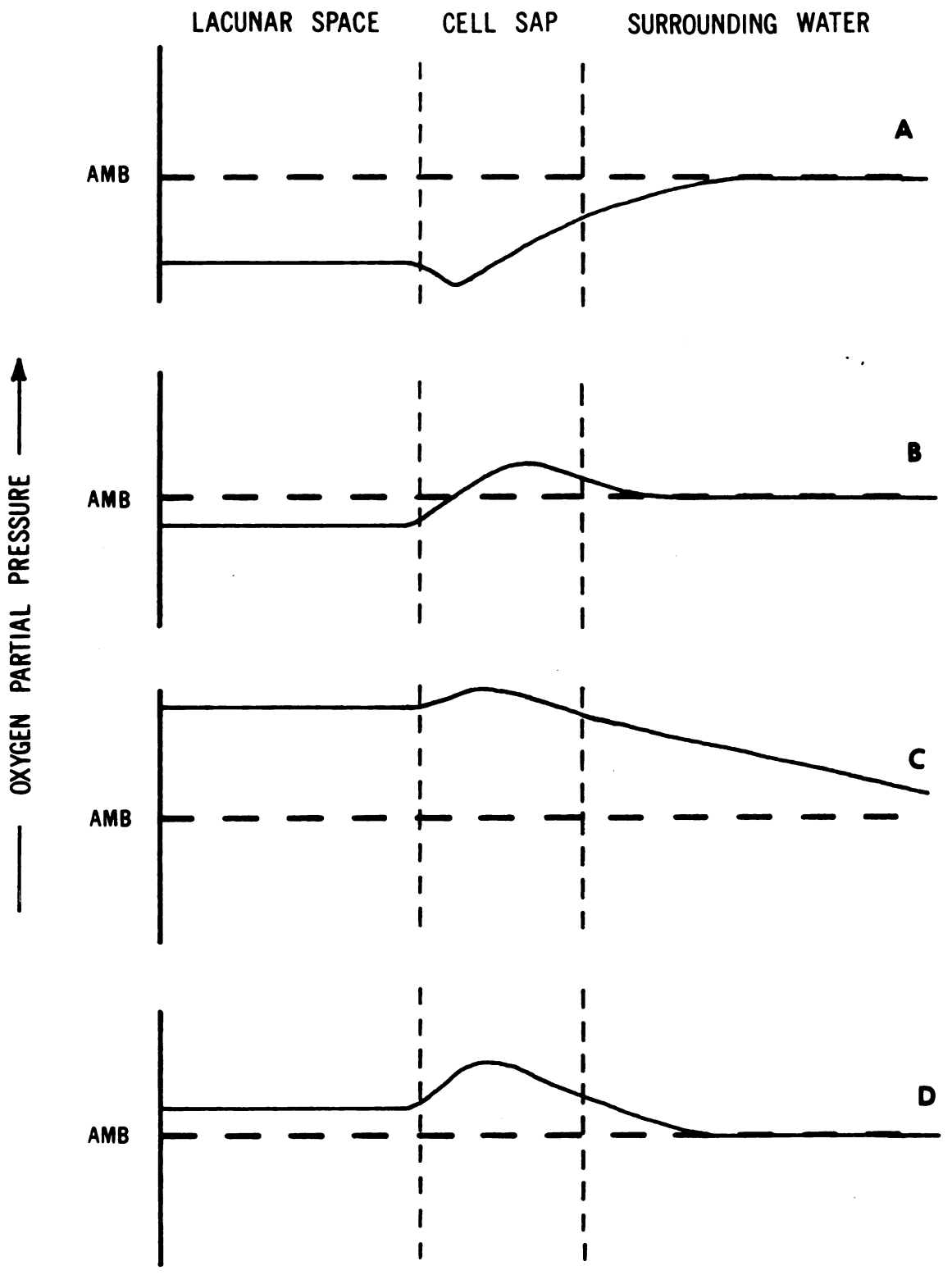
LACUNAR SPACE
CELL SAP
SURROUNDING WATER
A
AMB
B
AMB
C
AMB
D
AMB
OXYGEN PARTIAL PRESSURE

internal gas pressures could not have exceed 110 kPa, equivalent to the total pressure ($P_{atm} + P_h$) exerted at the 1 m depth. If the internal gas expanded, lacunar gas pressures would have been lower than 110 kPa. The shoots could not have initiated or maintained lacunar spaces at depths greater than 1 m on the strength of gas pressures alone.

Westlake (1978) determined oxygen content for lacunar spaces in *Myriophyllum spicatum* shoots grown at normal atmospheric pressure under saturating illumination (1,000 $\mu E \cdot m^{-2} \cdot sec^{-1}$ PAR). The mean of 9 observations was 21.9% O_2 with 2 samples at 28%. Again, lacunar gas pressures were too low to expand against hydrostatic pressure at depths greater than 1 m. Additionally, the low mean oxygen in lacunar gases probably resulted from stirring of the experimental chambers. This minimized the thickness of the boundary region, enhancing outward flux of oxygen as expected from the diffusive gas equilibrium model (cf. Figures 1C and 1D).

For an oxygen-induced lacunar air space at 20 C, the equilibrium oxygen concentration outside the plant surface increases five-fold from the surface to the 10 m depth. But net photosynthesis, required to maintain boundary layer oxygen levels, decreases rapidly from the surface downward, even in very clear lakes (cf. Golubic, 1963, for *Myriophyllum spicatum* in Lake Vrana). This concept is developed in Figure 2. In progressively deeper settings, lacunate hydrophytes should experience normal lacunar inflation throughout 24 hours, a zone in which photosynthetic oxygen efflux supports lacunar

Figure 2. Comparative values for equilibrium oxygen concentration outside an oxygen-induced gas space and net photosynthetic rate, relative to respective values at the water surface. Henry's Law shows equilibrium oxygen concentrations for submersed, oxygen-induced gas spaces increase five-fold from the water surface to 10 m depth. Decreases in net photosynthetic rate lower the oxygen concentration in boundary layer water, according to Fick's First Law.

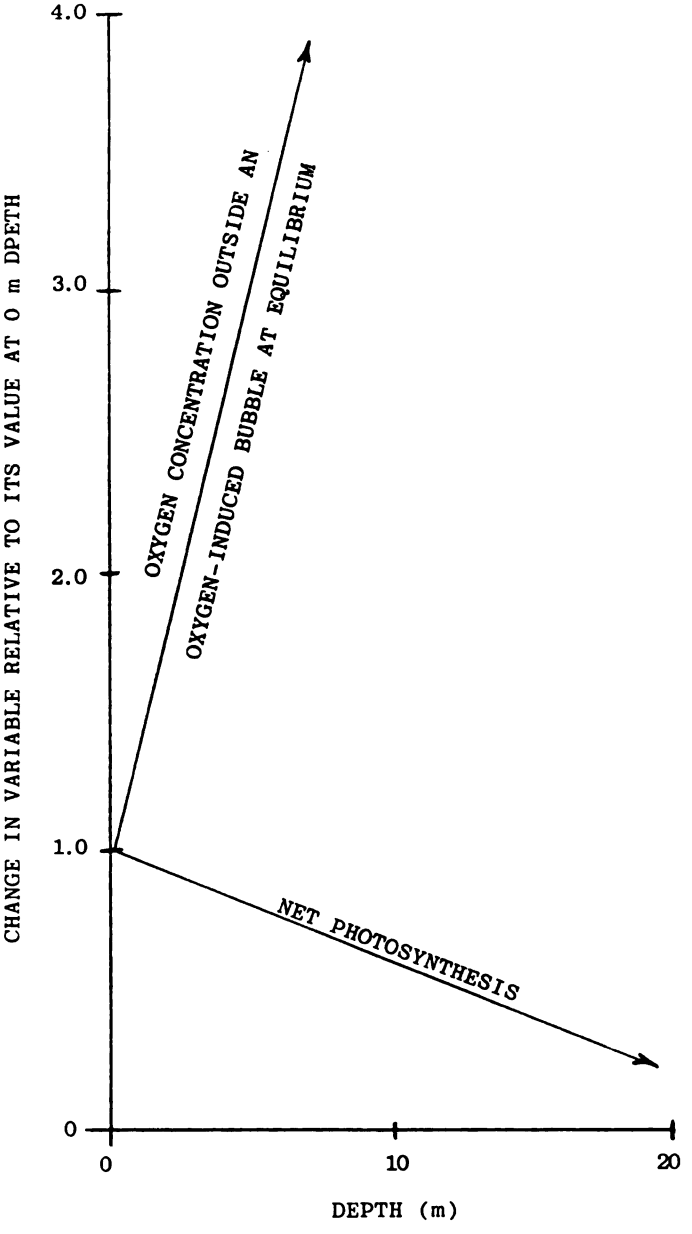
4.0
3.0
2.0
1.0
0
0
10
20
CHANGE IN VARIABLE RELATIVE TO ITS VALUE AT 0 m DPETH
DEPTH (m)
OXYGEN CONCENTRATION OUTSIDE AN
OXYGEN-INDUCED BUBBLE AT EQUILIBRIUM
NET PHOTOSYNTHESIS

inflation at mid-day (with deflation or collapse for the balance of the day), and a level below which lacunar inflation cannot be expected at any time. As a result of these considerations, the principle hypothesis of this research can be stated as follows:

> The partial pressure of oxygen in lacunar spaces of submersed hydrophytes is determined by the rate of net photosynthesis and the oxygen concentration in the water outside the plants' exterior surfaces. The diffusive demand on the plants' lacunar oxygen increases with lacunar oxygen partial pressure. Thus, net photosynthetic rates and boundary layer thickness determine a plant's ability to develop excess oxygen partial pressures which may be necessary to initiate schizogenous lacunae (cf. Dale, 1957) and to hold lacunar spaces open against the crushing forces of hydrostatic pressure. Moreover, the ability to store oxygen in lacunar spaces to meet dark respiration diminishes as hydrostatic pressure increases, as long as lacunar gas pressures reflect the prevailing hydrostatic pressures. Consequently, *hydrostatic pressure acts to limit the depth distribution of lacunate hydrophytes by restricting or eliminating the initiation and maintenance of lacunar gas spaces; a plant's ability to form and sustain schizogenous lacunar spaces at depth is determined by the net photosynthetic rate and the development of elevated oxygen concentrations in the epidermis and mesophyll cells and hence in the boundary region surrounding the plant.*

This hypothesis is attractive because it incorporates a plausible mechanism for hydrostatic pressure limitation of submersed vascular hydrophytes. The mechanism itself is attractive because it eliminates the need to invoke metabolic changes due to relatively small hydrostatic pressure loads. It also focuses on the lacunar spaces, the most obvious difference between plants which appear to be pressure-limited and those which seem to be unaffected by pressure. Lastly, the hypothesis entails the resolution of earlier, conflicting results on hydrostatic pressure limitation (Gessner, 1952; Fehrling, 1957; Bodkin, *et al.*, 1980; Dale,1981): it is essential that any experiments performed under hydrostatic pressure be conducted with atmospheric gas partial pressures outside the boundary region, just as plants likely experience in lakes.

Regarding this, Dale (1981) inappropriately utilized air pressure to develop total pressures in excess of 110 kPa in experiments on the possible limitation of *Myriophyllum spicatum* growth by hydrostatic pressure. Henry's Law clearly shows that dissolved gas levels surrounding plants in such an experiment are a function of the depth simulated. Most importantly, the diffusive demand in such a system would be similar to that at the water surface in a lake, regardless of the depth being simulated. There was no opportunity in Dale's (1981) experiments to exhibit a hydrostatic pressure influence on lacunar formation or function. Nonetheless, he concluded that hydrostatic pressure did not influence the

growth of *Myriophyllum spicatum*.

The static pressurization of remaining studies (Gessner, 1952; Fehrling, 1957; Bodkin, *et al.*, 1980) also placed plants under unrealistic gas balances. If dissolved inorganic carbon levels are sufficient, oxygen in closed, static systems may reach very high levels, possibly masking hydrostatic pressure effects. Experiments in which mercury manometers have been used to develop excess pressures (Gessner, 1952; Fehrling, 1957) may be further criticized for potential mercury toxicity to plants. Since mercury concentration in the water may be influenced by the pressure of mercury at the mercury/water interface, no adequate control can be established for such work.

A pressurization system was developed for this study which allowed control of gas levels and water flow rates in the vicinity of the plants. This system allowed realistic simulation of hydrostatic pressure and eliminated nuisance covariates.

Three basic questions were established to test the principle hypothesis:

1. *Is oxygen efflux during the light period influenced by hydrostatic pressure?* In metabolic studies by Vidaver (1972), hydrostatic pressure did not depress net photosynthetic rates at the 100-200 kPa level. But Hutchinson (1975) suggested that hydrostatic pressures as low as 50 kPa may depress net photosynthesis for some vascular hydrophytes.

2. *Does hydrostatic pressure decrease a plant's ability to store oxygen in its lacunae?* The dissolved gas equilibrium model shows that hydrostatic pressure can be expected to promote diffusive losses from oxygen-induced lacunar gas spaces.
3. *What is the normal structure of the lacunar system? Is it influenced by hydrostatic pressure?* As outward diffusion from plant tissues increases, the ability to form and sustain lacunar spaces decreases. Schizogenous lacunae held open by gas pressures alone should fail at relatively low hydrostatic pressures.

Myriophyllum spicatum was selected as the subject for tests performed during this research. Westlake (1978) measured lacunar volumes in this species as high as 15% of plant volume. This indicates that if lacunar volumes were diminished by the action of hydrostatic pressure, the change in gas balance may be observable. Lim (1976) measured root and shoot masses for dense stands of *Myriophyllum spicatum*. The mean root/shoot ratio for samples taken in late May was 2.7, suggesting that *Myriophyllum spicatum* must depend on lacunae to transport oxygen to its large root mass. Any inhibition of the lacunar formation or function can be expected to inhibit plant growth in natural settings.

METHODS AND MATERIALS

Experiments were conducted in a steel pressure chamber with acrylic windows. This unit is depicted in Figure 3. The walls and bottom of this tank were 6-mm mild steel plate, with 6 x 50-mm steel T-sections welded in place every 150 mm. All seams were reinforced by 6 x 25-mm steel angles, welded into the inside of the tank. A window frame was formed at the top of the tank by 6 x 38-mm steel angles welded just below the rim of the wall. These were welded so that a 90^0 angle was formed between the wall and the underside of the window frame. At 300-mm intervals, 6 x 50-mm steel T-sections were welded across the top of the window frame, on top of the angle rim. A flat 6 x 50-mm steel section was added to the underside of each T-section in order to make the underside of the window frame smooth and flat.

Windows were made from 15-mm acrylic plastic. The window at each end of the tank was permanently sealed in place with room-temperature vulcanizing rubber (RTV). A rubber gasket was placed under each of the center window frames, also sealed with RTV. These open frames served as access ports to the pressure tank. To close the tank, a light coat of stopcock grease was applied to the gasket and the windows

Figure 3. Diagrammatic representation of steel pressure chamber for control of hydrostatic pressure in experiments on oxygen efflux and influx for shoots of *Myriophyllum spicatum*. The tank accommodated 8 experimental enclosures. Water was removed from each enclosure through sampling tubes which led to the exterior of the tank.

TOP VIEW

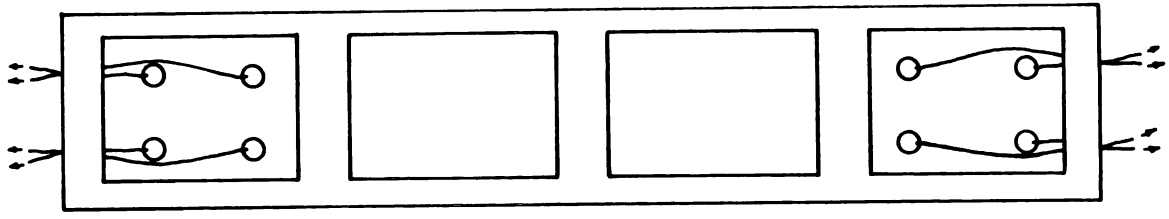

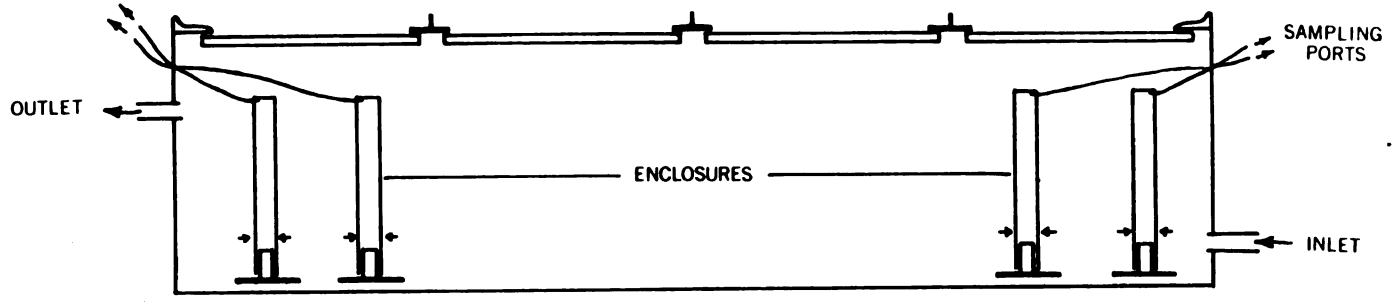

SIDE VIEW

were pulled into place with suction cups. Hydrostatic pressure from within the tank enforced the window seals.

A centrifugal pump pressurized the experimental tank, while providing a constant flow-through of water at 20 C and atmospheric gas saturation. The water flowed to the tank through plastic pipe. The outlet stream passed through fiber (particulate) and activated charcoal (dissolved organic carbon) filters on its way to a reservoir. The reservoir walls were insulated to maintain experimental temperatures. Continuous aeration by compressed air held dissolved gases in the reservoir at atmospheric saturation. A feed line from the reservoir to the pump completed the circuit.

Pressure in the experimental tank was controlled by balancing valves on the inlet and outlet streams, creating a velocity head in the tank. Pressure in the tank was measured by a standard air/water pressure gauge installed through the side wall of the tank. The average residence time for water in the tank was about 60 min. The tank was designed to be safe at 300 kPa above atmospheric pressure. An additional margin of safety was achieved by immersing the tank in a water-filled fiberglass chamber. Temperature control of the circulating immersion bath was used to maintain a 20 C experimental temperature.

Enclosing chambers were constructed to allow determination of apparent photosynthetic and respiratory rates of individual shoots of *Myriophyllum spicatum*. The chambers,

shown in Figure 4, were made from acrylic plastic tubing which was closed at the top by a thin disk of the same material welded in place by methylene chloride. The diameter of an enclosing chamber was slightly greater than that of the base unit tube. An enclosure slipped over the base unit as shown in Figure 4, and was sealed by an "O"-ring mounted at the top of the base unit tube. The enclosed volume was 150 ml. Water samples for oxygen analysis were removed from chambers through a 3-mm Tygon tube located at the top of the cylinder wall of each enclosure. This tube led through the wall of the pressure tank to the exterior. Four small (3-mm) holes, located in the side wall of the enclosing chamber just above the top of the base unit provided displacement water. The pressure tank accommodated 8 enclosures, 4 under each of the permanent windows. Water surrounding the enclosures in the experimental tank was sampled through a tube drawing water from the center of the tank. It led through the tank wall in the same fashion as the sampling tubes from the enclosures.

In order to determine hydrostatic pressure influence on net photosynthesis in *Myriophyllum spicatum*, net oxygen efflux rates were measured using the above enclosures. At the beginning of a period of measurement, enclosures and outlet tubes were flushed. Samples from the enclosures were then collected through the outlet tubes in 300 ml BOD bottles. A YSI probe and meter were used to confirm that the initial dissolved oxygen concentration in the enclosures

Figure 4. Enclosing chamber and base unit for measurement of oxygen efflux and influx for shoots of *Myriophyllum spicatum*.

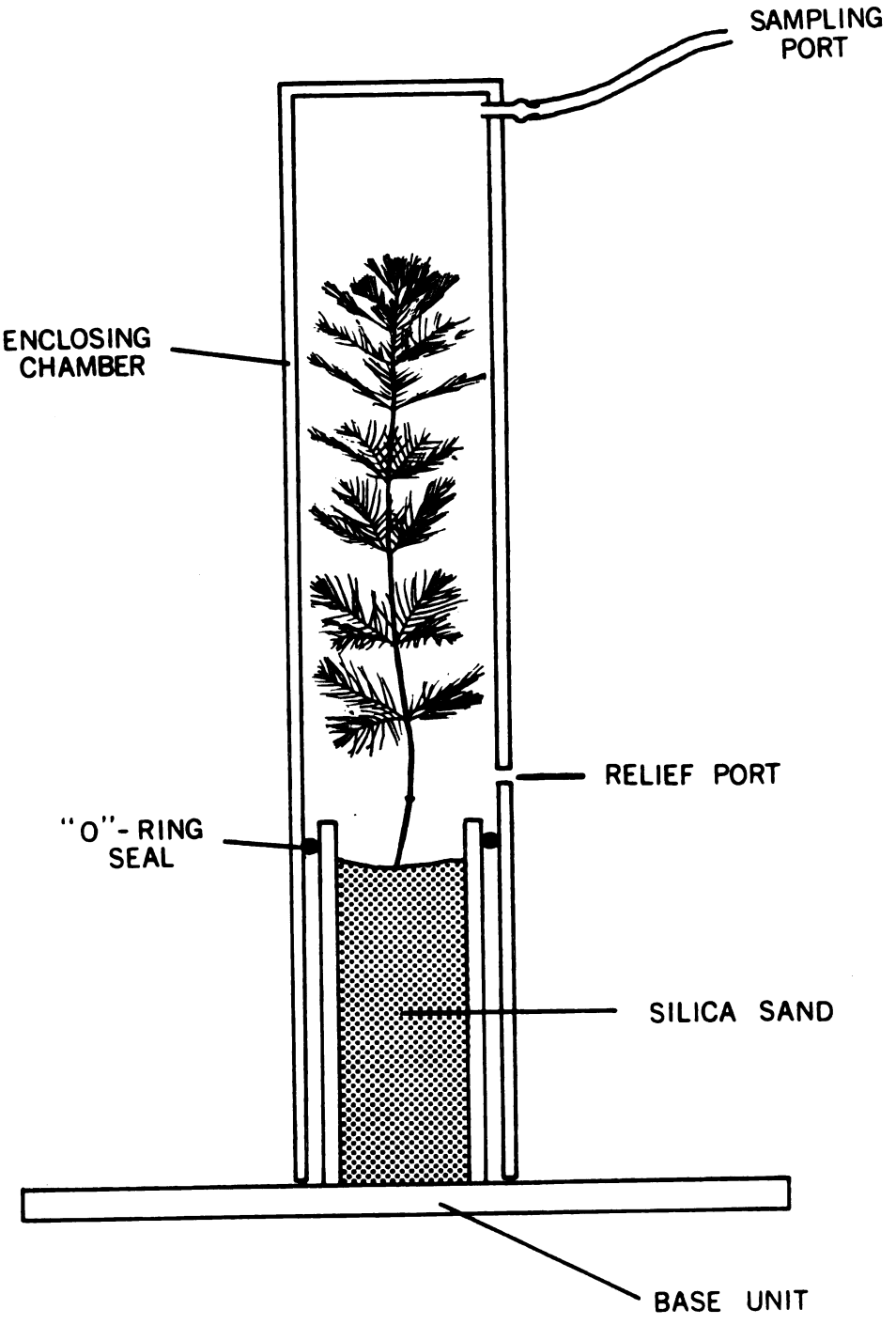
SAMPLING PORT
ENCLOSING CHAMBER
RELIEF PORT
"O"- RING SEAL
SILICA SAND
BASE UNIT

was at the saturation level for 20 C and atmospheric pressure (near 100 kPa). Outlet tubes were then clamped creating stagnant conditions in enclosures. Testing showed that measurable changes in oxygen concentration could be obtained with these enclosures using one-hour stagnation periods for shoots 10 cm or more in length. It was also found that in successive 300-ml samples from enclosures, the first sample showed deviation from ambient oxygen concentration, while the second and subsequent samples did not. This demonstrated that a 300-ml sample captured the oxygen produced during closure. The oxygen concentration in the 150 ml closure was then calculated from the concentrations in the 300 ml sample volume and the ambient sample as follows:

$$\underset{\text{(actual)}}{\text{ENCLOSURE } O_2} = 2 \cdot \underset{\text{(sample)}}{\text{ENCLOSURE } O_2} - \text{AMBIENT } O_2 \qquad \text{(EQN 7)}$$

The YSI system used to make these measurements was air-calibrated and checked against Winkler iodometric determinations (APHA, 1975).

Four pressures and four ranges of irradiance were used to measure the effect of hydrostatic pressure on net photosynthesis. A pressure 10 kPa above atmospheric was obtained by submersing enclosures at a depth of 0.1 m in an open circulating tank in the laboratory. Pressures 67, 100 and 152 kPa above atmospheric were established in the pressure tank to simulate water depths of 6.6, 10 and 15 m, respectively. Ranges of irradiance were obtained by placing

fiberglass screens that had been painted black between the light source and the windows of the pressure tank. Irradiance was mapped over locations occupied by enclosures using a Li-Cor portable PAR (photosynthetically active radiation) integrator and underwater sensor. A single light level of 104 $\mu E \cdot m^{-2} \cdot sec^{-1}$ was used for measurements at 0.1 m depth; 6 Sylvania VHO flourescent bulbs were the light source. Enclosures in the pressure tank were exposed to light ranges of 22-29, 47-68 and 115-174 $\mu E \cdot m^{-2} \cdot sec^{-1}$, under 2, 1 and 0 screens respectively. Lighting over the pressure tank was supplied by two 400-W high intensity discharge (HID) sodium lamps, suspended 1.5 m above the tank (cf., Appendix I). A 16 h light - 8 h dark cycle was maintained throughout all experiments.

A stock population of *Myriophyllum spicatum* has been maintained in outdoor ponds at the Limnological Research Laboratory at Michigan State University. This population developed from transplants from Lake Wingra, Dane County, Wisconsin, in 1973. Cuttings from outdoor ponds were planted into plastic trays filled with silica sand enriched with Ortho plant food pellets. These plants were used as a laboratory stock and were kept at 15 C with PAR at 80 $\mu E \cdot m^{-2} \cdot sec^{-1}$, on a 16 h light - 8 h dark cycle.

Active, low-algae shoot tips were cut from the laboratory stock to 10 cm lengths and planted into enclosure base units. The lower 2 cm of each shoot was buried in silica sand enriched with Ortho plant food pellets.

Plantings were placed in a recirculating nurturing bath at 20 C with PAR at 104 $\mu E \cdot m^{-2} \cdot sec^{-1}$, 16 h light - 8 h dark. The length and number of nodes were recorded for each shoot as it was placed in the nurturing system. Actively growing plants were used in experiments when they reached a length above the sand of 10 - 15 cm. This was normally 3 - 5 days after placement in the nurturing system.

A stock of 20-30 shoots was held in the nurturing system continuously. Inactive or algae-contaminated plants, and those which exceeded 15 cm in length were discarded. When algal contamination was evident on tank walls and many plants were affected, the entire shoot population was discarded. The experimental and nurturing systems were then bleached and the shoot population was re-established from the outdoor stock pond. Palmella stage *Chlamydomonas sp.* was the principle algal contaminant during these experiments.

Four groups of eight plants each were selected from the nurturing tank for experiments on the influence of light and pressure on net photosynthesis. Each group was tested at 10 kPa above atmospheric pressure with irradiance at 104 $\mu E \cdot m^{-2} \cdot sec^{-1}$, then was placed in the pressure tank to continue a sequence of treatment combinations at pressures 67 to 152 kPa above atmospheric. The sequence of treatments for each group is given in Table 1. Plants were acclimated under pressure for 24 h preceeding measurements. Chamber exit tubes remained open during acclimation to hold ambient gases in enclosures near atmospheric saturation. Net oxygen

Table 1. Summary of experiments conducted to determine the effect of hydrostatic pressure on net photosynthesis in *Myriophyllum spicatum*. Each group consisted of eight plants. For each experiment, the simulated depth (z) is given in meters; the range of irradiance (PAR) is given in $\mu E \cdot m^{-2} \cdot sec^{-1}$.

	EXPERIMENT									
	A		B		C		D		E	
GROUP	z	PAR	z	PAR	z	PAR	z	PAR	z	PAR
I	0.1	104	6.6	115-174	6.6	47-68	10	115-174	15	47-68
II	0.1	104	6.6	128-162	6.6	53-69	6.6	22-29	6.6	22-29
III	0.1	104	15	128-162	15	53-69	15	22-29		
IV	0.1	104	10	128-162	10	53-69	10	53-69	10	22-29

efflux measurements were taken during 1-h stagnation periods in all experiments except IV-E which was closed for 2 h. Chambers were flushed during the intervals between experiments to hold gases at saturation. Times between closures ranged from 15 to 67 minutes except experiments IV-D and IV-E for which the interval was 14 h (overnight).

After completion of net oxygen efflux measurements, each shoot was blotted dry and fresh weights were measured. The shoots were then extracted in dimethyl sulfoxide at 62 C for 1 h, following the method of Hiscox and Israelstam (1979). Chlorophyll-*a* of the extracts was calculated from the equations of Arnon (1949). Net oxygen efflux values (apparent photosynthesis) were recorded as $mgO_2 \cdot h^{-1} \cdot mg^{-1}$ Chl-*a*.

The influence of hydrostatic pressure on lacunar oxygen storage was determined by experiments on net oxygen influx rates (apparent respiration). The diffusion-controlled gas equilibrium model given in Figure 2 suggests that lacunar storage increases with increasing oxygen concentration outside the plant surface. Given this, the length of closure period at constant light would control the concentration of oxygen in the boundary region and hence the partial pressure of oxygen in the lacunae. By varying closure times we expected also to vary lacunar oxygen storage.

On the assumption that oxygen stored in the lacunae was more readily available to respiring tissues than oxygen in the surrounding water (cf. Hutchinson, 1975), we

expected to observe a reduced apparent respiration rate during dark periods as long as lacunar oxygen partial pressures were above those in the surrounding water. Preliminary experiments, reported in Appendix II, showed that apparent respiration rates were influenced by the ambient oxygen concentration reached during the preceeding photosynthetic period. In order to test the expectation that hydrostatic pressure would reduce lacunar oxygen storage, two groups of eight plants each were entered into the experimental closures, one at 67 kPa above atmospheric pressure and the other at 152 kPa above atmospheric pressure, simulating the 6.6 and 15 m depths, respectively. Six of the eight enclosures were sealed at times ranging from 3 to 10 h before darkness to achieve a broad range of final oxygen concentrations in the water surrounding the individual shoots. The remaining two chambers were left flowing throughout the light period so gases in the water surrounding these shoots would remain at atmospheric saturation. At the end of the light period the tank was covered with aluminum foil and 3-300 ml sample volumes were withdrawn from each enclosure. Flow through the chambers was then closed. A single 300 ml sample was withdrawn hourly from each enclosure during the dark period. A sample was drawn from the ambient tap in the pressure tank at each sampling time. All samples were analyzed for dissolved oxygen by the Winkler iodometric method (APHA, 1975) with the titrant strength reduced to half to improve the precision of the measurements.

The oxygen concentration in the first of the three samples drawn at the end of the light period was used to estimate the final oxygen concentration in the water surrounding each shoot. The second and third samples were analyzed to ensure that the chambers had returned to atmospheric oxygen levels prior to the start of respiration measurements. The preliminary experiments suggested that only the first of the hourly respiration measurements was likely to be influenced by lacunar storage. Also, there was an indication that respiration may decrease near the end of an 8 h dark period. Given this, basal respiration was estimated by the mean of hourly rates observed during the second through sixth hours of darkness. The lacunar storage (LS) of oxygen was then estimated as the relative decrease in apparent respiration seen during the first hour of darkness when compared to the basal rate established during hours 2 through 6 of darkness. This index value was calculated as follows:

$$LS = \frac{\overline{I}_{2-6} - I_1}{\overline{I}_{2-6}} \qquad \text{(EQN 8)}$$

where I_1 is the apparent respiration for the first hour of darkness and $\overline{I}_{2-6}$ is the basal rate from hours 2 through 6. Notice that in the case where the respiration during hour 1 equals the basal rate, the value for LS is 0. If the value for I_1 is 0, LS is 1.0. In a case where oxygen continues to exit the plant during the first hour of darkness, I_1 becomes negative and LS is greater than 1.

Following sample withdrawl for the eighth hour of dark respiration, the foil covering was removed from the tank and hourly sample withdrawl was continued through the light period. No flushing was allowed between these closure periods. The results of these tests were used to assess the stability of oxygen efflux under constant light. The 67 kPa group was blotted dry and weighed then oven-dried to constant weight at 105 C for fresh/dry weight ratio estimates and to allow estimation of dark respiration rates on a dry weight basis. These estimates were coupled with earlier net photosynthesis results to allow predictions of 24-h compensation depths.

Plants were grown at 0.3 and 8-m depth simulations to examine the influence of hydrostatic pressure on the internal anatomy of *Myriophyllum spicatum*. Plants at 0.3 m were held in standard nurturing conditions throughout their growth period. Eight plants, 5 cm in length, were taken from the 0.3-m population and planted into the experimental tank. The tank was then pressurized to the 8-m depth. When plants reached 15 cm, they were removed after slow decompression. The upper 10 cm of each shoot was removed, representing growth which occurred at the 8 m depth. At this time a group of plants was also removed from the 0.3-m population. Plant sections were fixed in FAA.

Representative shoot sections were selected from each experimental group; leaves, stems and roots were separated. These were dehydrated and embedded in Paraplast following

the outline of Sass (1951). Serial sections were made with an IEC rotary microtome. Apical sections were taken at 10-µm intervals; leaflet, rachis, lower stem and root sections were made at 20-µm intervals. Paraplast ribbons were mounted on slides with a gelatin/water/formalin adhesive (Sass, *Ibid.*). Slides were labelled to maintain serial order of the sections. The Paraplast was removed with xylene. Safranin was used as the primary stain with a 30-min exposure. Fast green provided a counterstain at 30-sec exposure. The slides were completed by the placement of a cover slip affixed by Permount.

Sections from the two groups were compared to determine whether hydrostatic pressure influenced the lacunar structure. The anatomy of both groups were compared to the *Myriophyllum spicatum* sections shown in Hasman and Inanc (1957). Particular attention was given to lacunar development in the shoot apices since this information is not available in the literature.

Mature *Myriophyllum spicatum* shoots may grow to lengths in excess of 4 m. The base of these stems are much larger than any which could be grown in this experimental study. To examine the anatomy of mature stem sections, plants were harvested from the 2-m depth in the outdoor stock pond. Sections from the base of these plants were prepared for examination under a scanning electron microscope (SEM) by gluteraldehyde fixation and critical point drying. The sections were examined under SEM at the Center for Electron

Optics at Michigan State University. The results of this exercise were combined with light microscope examination of the Paraplast sections to determine the structure and continuity of the lacunar system for the entire plant.

RESULTS

NET OXYGEN EFFLUX MEASURMENTS

Data regarding the influence of light and pressure on net oxygen efflux for each experimental treatment used in this study are given in Appendix III. Figure 5 shows combined results from all treatments. At 10 kPa above atmospheric pressure with PAR at 104 $\mu E \cdot m^{-2} \cdot sec^{-1}$, the mean net oxygen efflux (NOE) for all shoots was 1.25 $mgO_2 \cdot h^{-1} \cdot mg^{-1}$ Chl-*a*, the standard error of the mean estimate was 0.056 with n = 31. The results of measurments made at the three high pressures were combined by pressure level and summarized by logarithmic regression equations. At 67 kPa above atmospheric pressure,

$$NOE = -2.50 + 0.82 \cdot \ln(PAR) \qquad (r^2 = 0.93) \qquad (EQN\ 9)$$

at 101 kPa above atmospheric pressure,

$$NOE = -2.19 + 0.68 \cdot \ln(PAR) \qquad (r^2 = 0.92) \qquad (EQN\ 10)$$

and at 152 kPa above atmospheric pressure,

$$NOE = -2.68 + 0.86 \cdot \ln(PAR) \qquad (r^2 = 0.95) \qquad (EQN\ 11)$$

where NOE values are given in $mgO_2 \cdot h^{-1} \cdot mg^{-1}$Chl-*a* and PAR values are in $\mu E \cdot m^{-2} \cdot sec^{-1}$. The r^2 value is the coefficient of determination for the fit of the logarithmic curve.

The plot of logarithmic equations shown in Figure 6 suggests that the plants grown at 67 and 152 kPa above atmospheric pressure were similar in their photosynthetic

Figure 5. Net oxygen efflux for *Myriophyllum spicatum* shoots as a function of photosynthetically active radiation (PAR) at 10 (⬡), 67 (○), 101 (△) and 152 (□) kPa above atmospheric pressure.

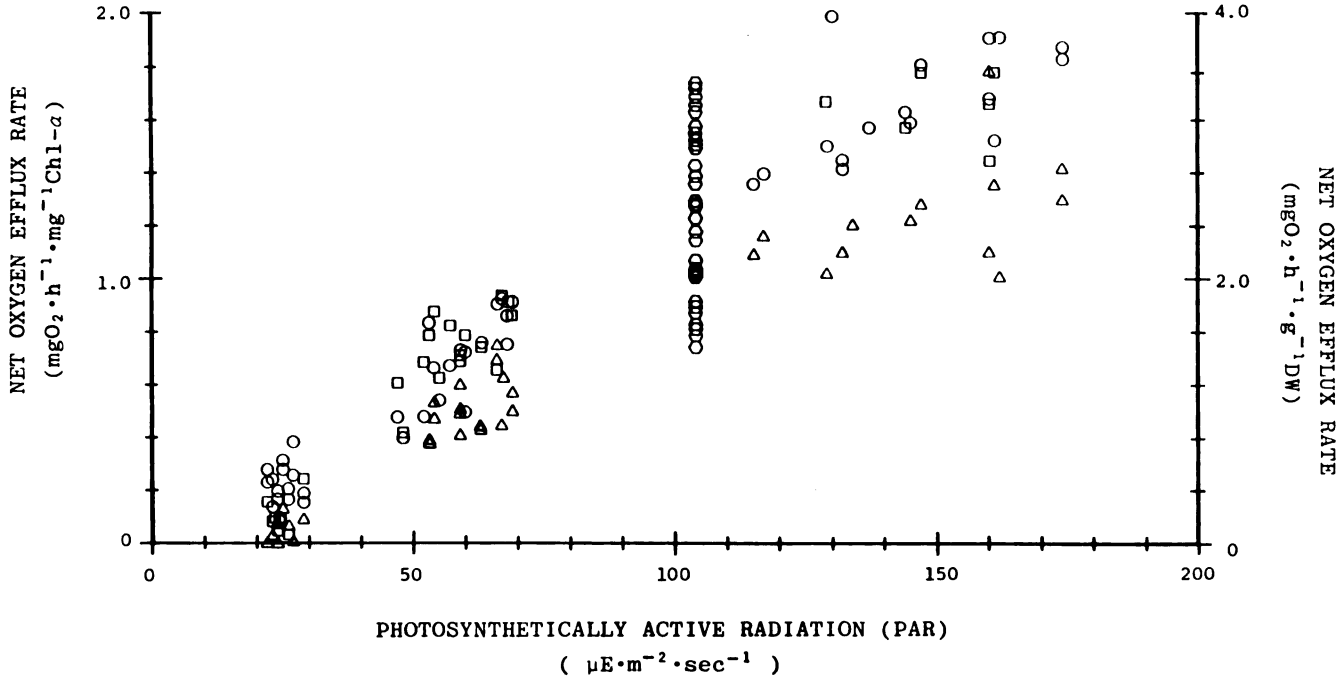
NET OXYGEN EFFLUX RATE
(mgO2·h-1·mg-1Chl-a)
2.0
1.0
0
0
50
100
150
200
4.0
2.0
0
NET OXYGEN EFFLUX RATE
(mgO2·h-1·g-1DW)
PHOTOSYNTHETICALLY ACTIVE RADIATION (PAR)
(μE·m-2·sec-1)

Figure 6. Logarithmic regression curves for net oxygen efflux in *Myriophyllum spicatum* shoots as a function of photosynthetically active radiation (PAR) at 67 (○), 101 (△) and 152 (□) kPa above atmospheric pressure.

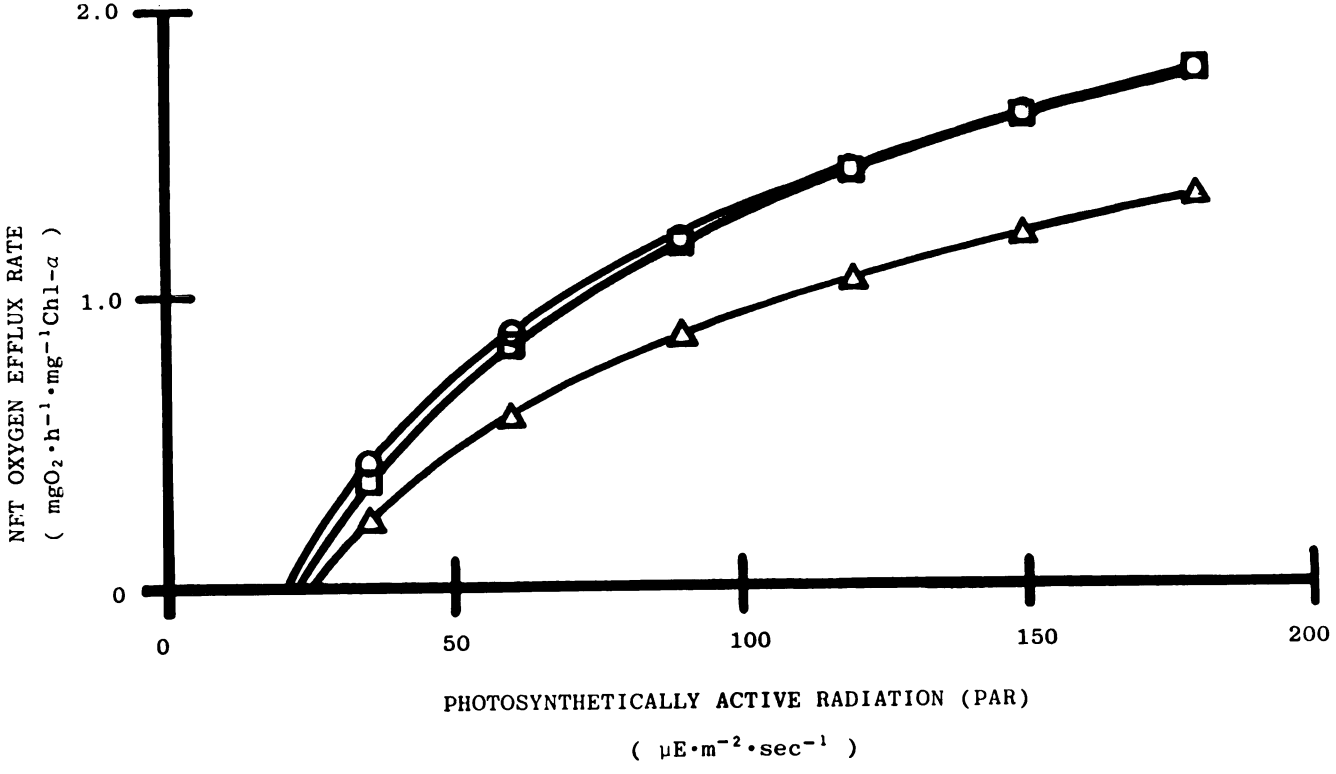
2.0
1.0
0
NET OXYGEN EFFLUX RATE
($mgO_2 \cdot h^{-1} \cdot mg^{-1}Chl\text{-}a$)
0
50
100
150
200
PHOTOSYNTHETICALLY ACTIVE RADIATION (PAR)
($\mu E \cdot m^{-2} \cdot sec^{-1}$)

Figure 7. The time lag for reaching steady net oxygen efflux following changes in light level during the treatment sequence I-B•I-C•I-D . Values shown are treatment means plotted at the mean light level; bars indicate 90% confidence limits. Similar patterns were observed in sequences I-C•I-D•I-E , II-C•II-D•II-E and IV-B•IV-C•IV-D . The solid line indicates the logarithmic curve for the 67 and 152 kPa experimental groups.

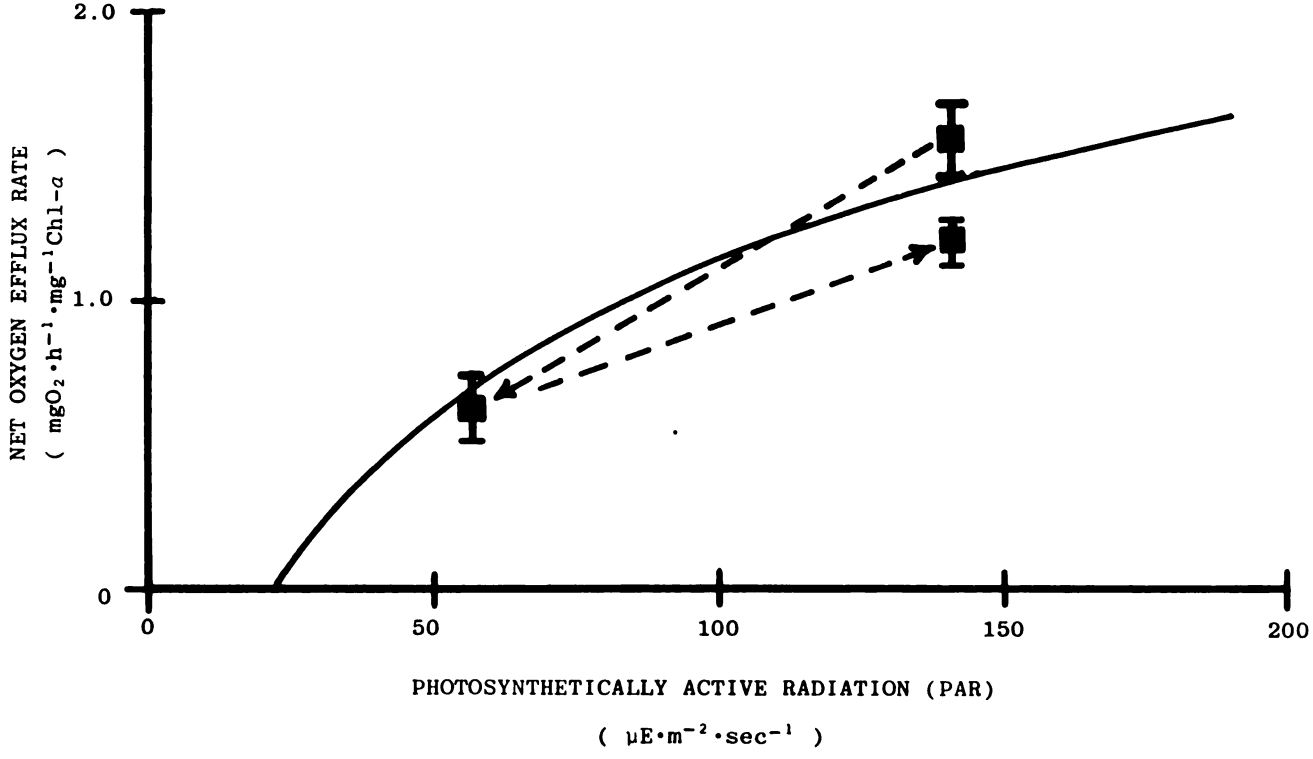
2.0
1.0
0
NET OXYGEN EFFLUX RATE
($mgO_2 \cdot h^{-1} \cdot mg^{-1}Chl\text{-}a$)
0
50
100
150
200
PHOTOSYNTHETICALLY ACTIVE RADIATION (PAR)
($\mu E \cdot m^{-2} \cdot sec^{-1}$)

response to light. Plants grown at 101 kPa above atmospheric pressure had a lower light response. From these data, hydrostatic pressure could not be shown to influence net oxygen efflux in shoots of *Myriophyllum spicatum*. Although the results from 101 kPa above atmospheric pressure were lower than the other three pressures, hydrostatic pressure was expected to act in a continuous manner, diminishing the photosynthetic response at 152 kPa above atmospheric pressure at least to the extent that the 101 kPa plants were influenced.

Two factors other than hydrostatic pressure may have contributed to the lowered net oxygen efflux estimates in the shoots grown at 101 kPa above atmospheric pressure. The mean chlorophyll content per gram fresh weight (FW) was lower for experimental Group IV than for any of the other plant groups (cf. Appendix III). There also appears to have been a long lag-time for re-establishing steady net oxygen efflux rates after changes in light level during experiments. An example of this is shown in Figure 7, where treatment I-D (101 kPa) may have inadvertently been influenced by the earlier NOE rate established at a lower light level. This equilibration pattern was anticipated in the diffusive gas equilibrium model shown earlier in Figure 2. However, the minimum 15 min flushing time was originally thought to be adequate to return the lacunar compartment to atmospheric equilibrium.

Points from the logarithmic prediction equations were

entered into the Lineweaver-Burke double-reciprocal plot to estimate kinetic coefficients at 20 C. Since the curves did not pass through the origin, the value $1/(PAR - PAR_C)$ was substituted for $1/(PAR)$, where PAR was the actual light (i.e. substrate) level and PAR_C was the light compensation point for net oxygen efflux, estimated by the X-intercept from the logarithmic plots. This procedure shifts the Y-axis in the Michaelis-Menton kinetics plot to the compensation point. The resulting kinetic constants were as follows for combined data from 67 and 152 kPa above atmospheric pressure:

$$V_{max} \text{ for NOE} = 2.13 \text{ mgO}_2 \cdot h^{-1} \cdot mg^{-1} \text{ Chl-}a$$

$$K_m \text{ for light} = 75 \ \mu E \cdot m^{-2} \cdot sec^{-1}$$

$$\text{Light compensation for NOE} = 21 \ \mu E \cdot m^{-2} \cdot sec^{-1} \ .$$

For data from 101 kPa above atmospheric pressure:

$$V_{max} \text{ for NOE} = 1.79 \text{ mgO}_2 \cdot h^{-1} \cdot mg^{-1} \text{Chl-}a$$

$$K_m \text{ for light} = 92 \ \mu E \cdot m^{-2} \cdot sec^{-1}$$

$$\text{Light compensation for NOE} = 25 \ \mu E \cdot m^{-2} \cdot sec^{-1} \ .$$

The net oxygen efflux (apparent photosynthesis) from shoots of *Myriophyllum spicatum* can be modelled as follows:

$$NOE = V_{max} \cdot \frac{(PAR - PAR_C)}{K_m + (PAR - PAR_C)} \qquad \text{(EQN 12)}$$

Equation 12 follows the general form of the Michaelis-Menton enzyme kinetic equation, with the Y-axis shifted to the light compensation point for net oxygen efflux.

LACUNAR OXYGEN STORAGE ESTIMATES

Lacunar storage of oxygen (LS) was estimated for plants at 67 and 152 kPa above atmospheric pressure by depression of net oxygen influx (apparent respiration) as described in Equation 8, above. The results of these experiments are shown in Figure 8, and are tabulated in Appendix III. Storage at 67 kPa above atmospheric ranged from 0 to 1.0 with ambient oxygen concentrations ranging from 8.1 to 31.7 $mgO_2 \cdot l^{-1}$. A logarithmic curve was fitted to these data as follows:

$$LS = -0.73 + 0.49 \cdot \ln(O_2) \qquad (r^2 = 0.75) \qquad \text{(EQN 13)}$$

As expected, these results demonstrated the existence of a relation between oxygen storage in the lacunae and oxygen concentrations in the surrounding water.

Storage at 152 kPa above atmospheric pressure ranged from -0.22 to 1.0 with external oxygen concentrations from 8.1 to 20.4 $mgO_2 \cdot l^{-1}$. A logarithmic curve was established for these data:

$$LS = -1.35 + 0.68 \cdot \ln(O_2) \qquad (r^2 = 0.38) \qquad \text{(EQN 14)}$$

The comparison of these two groups of data does not support the hypothesis that hydrostatic pressure decreases lacunar oxygen storage by enhancing outward diffusion.

Fresh and dry weights (DW) were determined for the group of plants tested at 67 kPa above atmospheric pressure. Respiration and photosynthesis values for these experiments were normalized by gDW and are tabulated in Appendix III. The mean respiration rate for the second through sixth

Figure 8. Estimates of lacunar oxygen storage as a function of dissolved oxygen concentration in the water surrounding shoots of *Myriophyllum spicatum* at 67 (○) and 152 (△) kPa above atmospheric pressure.

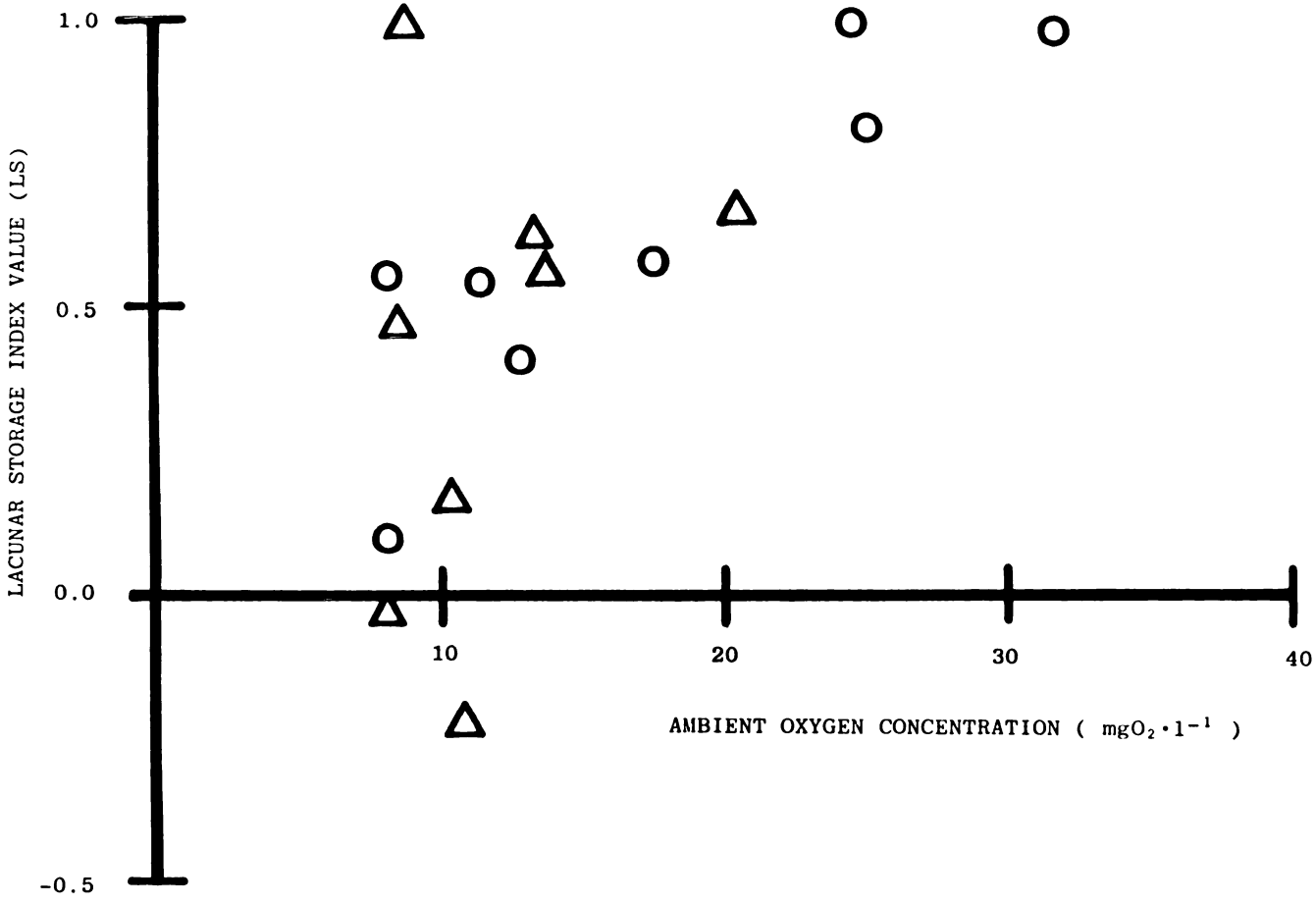
1.0
0.5
0.0
-0.5
LACUNAR STORAGE INDEX VALUE (LS)
10
20
30
40
AMBIENT OXYGEN CONCENTRATION ($mgO_2 \cdot l^{-1}$)

hours of darkness was 0.872 $mgO_2 \cdot h^{-1} \cdot g^{-1}DW$; the standard error for the mean estimate was 0.038 with n = 40. FW/DW and Chl-*a*/FW ratios were calculated from shoots involved in lacunar storage and net oxygen efflux experiments, respectively. These calculations showed approximately 2.005 mgChl-*a*/gDW . Based on this conversion factor, the net oxygen efflux rates during the photosynthetic period of the lacunar storage experiment were similar to those of the 67 and 152 kPa results reported in Figures 6 and 7.

LACUNAR STRUCTURE

Paraplast thin sections were made from shoots grown at pressures equivalent to 0.3 and 8 m depths. No differences in internal anatomy could be determined from sections of these two experimental groups. All leaflet, rachis, stem and root sections had normal morphological organization as shown by comparison with the anatomy of *Myriophyllum spicatum* given by Hasman and Inanc (1957). Representative sections were photographed under the light microscope and are shown in Appendix IV.

Lacunar development was assesed from apical sections, sections taken 10 cm below the shoot apex, and sections taken 2 m below the apex. Experimental plants were used for apical and 10-cm sections. Specimens for the 2-m sections were collected from outdoor stock ponds, and sections were made at the position just above the sediment surface. Figure 9 depicts the lacunar development in the apical

Figure 9 . Development of lacunar spaces in the meristem region of *Myriophyllum spicatum*. A. Apical cells, 0.04 mm below shoot apex; B. Transverse stem cross-section, 0.4 mm below shoot apex; C. Transverse stem cross-section, 0.7 mm below shoot apex; D. Detail of C, showing septum cells.

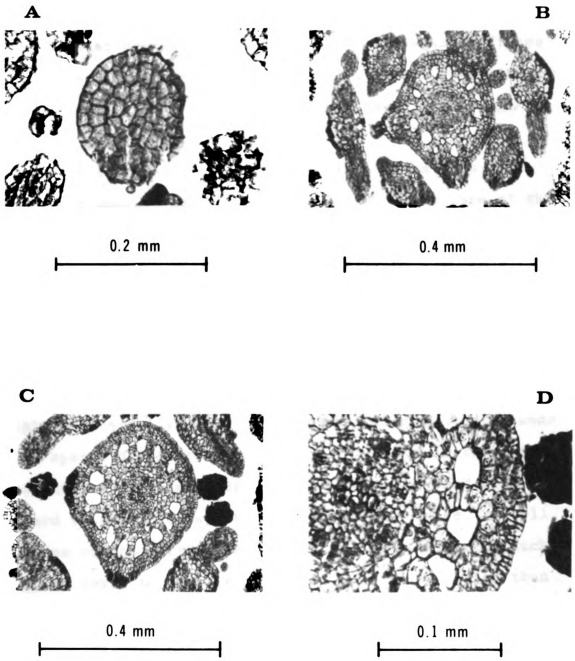
A
B
0.2 mm
0.4 mm
C
D
0.4 mm
0.1 mm

region. Tissues were poorly defined 40 µm below the shoot apex (Figure 9a). Lacunae first began to open at 200 µm below the apex; the 15 lacunae seen in mature stems were all at least partially open 400 µm below the apex (Figure 9b). The lacunar architecture seen in mature stem sections was clearly evident 700 µm below the apex. This stage is shown in Figures 9c and 9d.

Stem sections taken 10 cm below the apex were about 1 mm in diameter, as shown in Figure 10. Structure of the cortex in this region of the stem is depicted in Figure 11. Each lacuna has a distinct arch of cells on the inner and outer radii. Lacunae are bounded on the sides by *septae* which have a *load collector* cell at the end joining two *outer arches*, and a *load distributor* cell on the inside joining two *inner arches*. Given a uniform radial load applied externally (eg., hydrostatic pressure) the *lacunar arch system* dissipates a portion of the load in the outer and inner arches and redirects the remaining load safely inward to avoid collapsing the lacunar air space. In all regions of the cortex, the external load is directed such that it tends to push cells toward each other rather than pulling them apart. In a fashion analogous to the *lacunar arch system*, the strength of arches in ancient Roman bridges was determined by the strength of the bricks rather than the mortar.

Sections from 2 m below the shoot apex were taken from the outdoor stock pond and examined under a scanning electron

Figure 10. Transverse cross-section through stem of *Myriophyllum spciatum*. Section taken 10 cm below shoot apex.

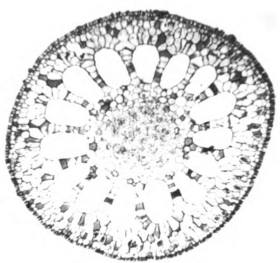

1 mm

Figure 11. The *lacunar arch system* in the cortex of *Myriophyllum spicatum* stems.

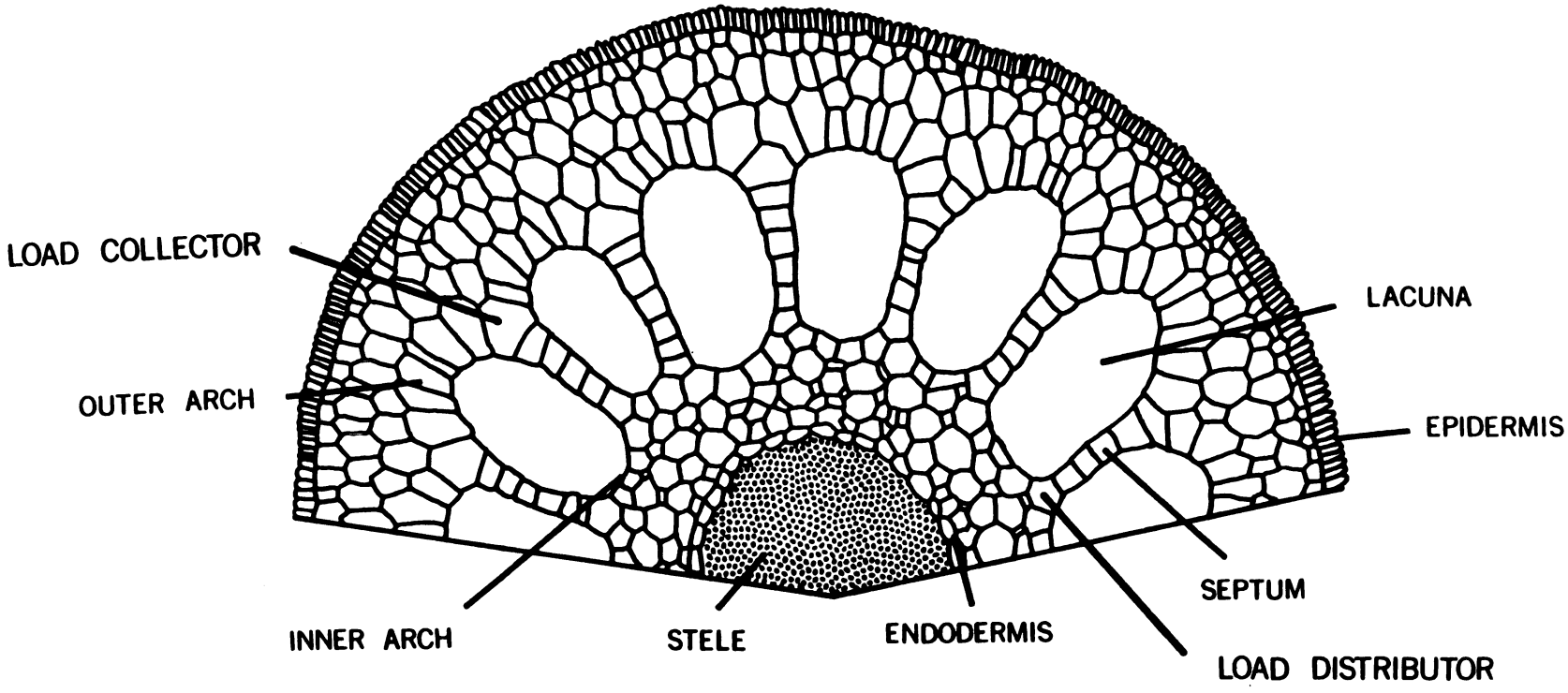
LOAD COLLECTOR
OUTER ARCH
INNER ARCH
STELE
ENDODERMIS
SEPTUM
LOAD DISTRIBUTOR
LACUNA
EPIDERMIS

microscope (SEM). These sections were approximately 2 mm in diameter; one is shown in Figure 12. In this region of the stem, the *septae* are long and thin and the *outer arches* are expanded, diminishing the load-distributing character of the *lacunar arch system* relative to that seen in the younger stems. Hasman and Inanc (1957) show the presence of storied cork in mature stems of *Myriophyllum spicatum*. The presence of storied cork cannot be confirmed for the mature sections in this study since SEM procedures do not distinguish secondary tissues. If present, however, storied cork would enhance the strength of the stem against crushing forces.

The continuity of the lacunar system was determined from the Paraplast sections shown in Appendix IV. No connection was found between lacunae in the leaflets, rachis and stem sections. Along the stem, the lacunar system was continuous except for partial interruptions by vascular leaf traces at the nodes. In stem sections where adventitious roots had developed, blockage of lacunae by roots was substantial. It is important to note, however, that adventitious roots are usually only present in shoots beginning to fragment from the parent plant.

Figure 12. Stem cross-section of *Myriophyllum spicatum* taken 2 m below the apex. Examined under scanning electron microscope at the Center for Electron Optics at Michigan State University.

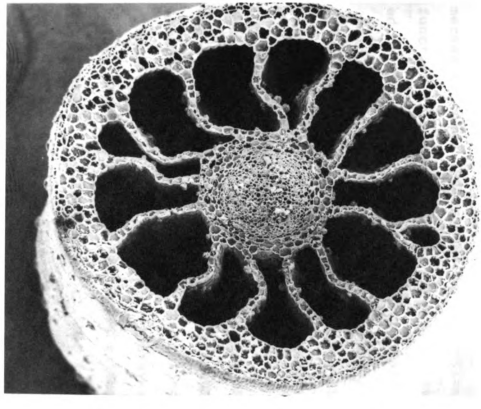

1 mm

DISCUSSION

The principle hypothesis in this work held that hydrostatic pressure should limit the depth distribution of submersed vascular hydrophytes by preventing the formation and function of lacunar spaces. The hypothesis was not supported by the results of this research; hydrostatic pressure could not be shown to influence *Myriophyllum spicatum* shoots in any of the observations made during this study. Three issues must be pursued based on the observations given above; (1) gas balances behaved as predicted by the diffusive gas equilibrium model, (2) the observation that lacunar storage was not diminished by hydrostatic pressure suggests that lacunar gas pressures were not controlled by hydrostatic pressure, and (3) the influence of hydrostatic pressure on mature shoots may not be reflected in the performance of young shoots like those used in this study.

Two groups of observations supported the diffusive gas equilibrium model. During net oxygen efflux experiments a time-lag for equilibration of oxygen efflux occurred following changes in light level. This was shown in Figure 7. The diffusive gas equilibrium model showed that a back-pressure for oxygen movement must be established as oxygen exits plant surfaces, allowing accumulation of oxygen in lacunar

air spaces. Any change in light level caused a like change in the net photosynthetic rate and a concomitant change in back-pressure for oxygen accumulation. Before stable oxygen efflux was achieved, the boundary region and lacunar air spaces must have reached equilibrium oxygen levels. In the case of decreasing light between experiments, this entailed unloading of the lacunae, cell sap and boundary region oxygen to the new, lower oxygen equilibrium levels. Oxygen efflux during unloading was higher than the net photosynthetic rate. Following an increase in light, oxygen efflux was lower than the net photosynthetic rate until the system was loaded to its equilibrium level. This followed from Equation 6; stable efflux was not achieved until the Δ CONCENTRATION value reached its equilibrium level following filling of the gradient with oxygen.

Westlake (1978) observed similar equilibration lags in *Myriophyllum spicatum* and *Vallisneria americana* Michx., both lacunate hydrophytes. Net oxygen efflux values were initially depressed following the start of a light period. After a mean lag of 9.5 min, stable oxygen efflux was observed. Equilibration lags were also observed following rapid flushing with water at atmospheric saturation. Breakdown of the still boundary region forced unloading of the lacunae, cell sap and boundary region oxygen. After flushing was complete, oxygen efflux lagged while oxygen levels were re-established in the three compartments.

The relation between ambient oxygen concentration and

lacunar storage indices developed in this study also followed from the diffusive gas equilibrium model. By allowing oxygen levels in the boundary region to build during extended stagnation, back-pressure for lacunar oxygen storage increased. These results confirm the notion that lacunar oxygen storage should be enhanced in stagnant waters where boundary layer thickness is greater than in flowing water. For example, lacunar storage must be enhanced in the massive mats of *Myriophyllum spicatum* which appear near the water surface in summer.

Given the diffusive gas equilibrium model, it was expected that hydrostatic pressure would act to diminish or eliminate lacunar gas storage. This prediction was based on the notion that gases would exit the lacunar spaces whenever internal gas partial pressures exceeded partial pressures at a plant's exterior surface. If internal gas pressures were determined by hydrostatic pressure as suggested in the literature (cf. Dale, 1957; Sculthorpe, 1967), outward diffusion would have depleted lacunar oxygen levels, except possibly at the highest net photosynthetic rates. Failure of this prediction forced consideration of the possibility that lacunar gas pressures were independent of prevailing hydrostatic pressures.

Dale (1957) showed that rates of lacunar formation in the apical region of *Elodea canadensis* were directly related to illumination. Dale (*Ibid.*) and Sculthorpe (1967) concluded that oxygen evolved by the photosynthetic hydrolysis

of water pressurized lacunae and forced their expansion. To force expansion at depth, lacunar gas pressures must exceed total pressures ($P_{atm} + P_h$) forcing inward on plant surfaces. But it is also possible that growth of cells in the apical region causes lacunar formation. If cells in the apex were appropriately positioned and shaped, expansion of the cells by turgor pressure during normal growth processes would form and expand lacunar spaces. Dale (1957) and Sculthorpe (1967) did not give cross-sectional anatomy for developing *Elodea canadensis* apices. However, shoot apices of *Myriophyllum spicatum* examined during this study showed a distinctive cellular arrangement, the lacunar arch system. The lacunar arch structure may force expansion of lacunar spaces without gas pressurization.

Septae in stem sections of *Myriophyllum spicatum* enlarged primarily by cell expansion and to a lesser extent by cell division. At 0.7 mm below the shoot apex (Figures 9C and 9D) the septum was composed of 3-4 cells averaging 3 µm in length along the stem radius. Septae from 10 cm below the apex were composed of 4-5 cells, 25 µm in length (Figure 10). Sections from outdoor stock ponds taken 2 m below the shoot apex had septae composed of 9-10 cells averaging 35 µm in length along the stem radius (Figure 12). Cell expansion is driven by turgor pressurization combined with relaxation of cell wall fibers (Salisbury and Ross, 1978). Sculthorpe (1967) pointed out that cell turgor pressures are generally high in young hydrophyte tissues, increasing as metabolic

activities elevate sugar and ion levels. Turgor-driven cell expansion can progress independently from gas pressurization of lacunar spaces. Increased metabolic activity associated with increased illumination may explain the correlation between illumination and lacunar expansion rates found in *Elodea canadensis* by Dale (1957).

The lacunar arch system in *Myriophyllum spicatum* allows the expansions and divisions of lacunar development to proceed against substantial external loads. In this study, normal lacunar development was observed in shoots grown under 83 kPa hydrostatic pressure. As long as the lacunar arch system dissipates hydrostatic pressure loads, stems of *Myriophyllum spicatum* should be able to maintain lacunar gas pressures near atmospheric levels (101 kPa), regardless of their depth of immersion.

Lacunae in leaf tissues of *Myriophyllum spicatum* were not as well developed as stem lacunae. But oxygen efflux measurments made during this study provide evidence that leaf lacunar gas pressures also could not have matched prevailing hydrostatic pressures. Equation 6 showed that magnitude of the oxygen gradient at steady state, Δ CONCENTRATION (ΔC), is determined by efflux of oxygen from a specified surface area and resistance to oxygen movement, R, through the boundary region. Having made net oxygen efflux measurements for shoots of *Myriophyllum spicatum*, it is only necessary to specify values for the remaining variables in Equation 6 to estimate values for ΔC.

According to Campbell (1977), resistance to gas movement, R, is a function of thickness of the boundary region, shape of the diffusing body and the diffusion coefficient for oxygen in water. For a leaflet of *Myriophyllum spicatum* (a cylindrical source),

$$R = \frac{a}{D} \cdot \ln\frac{b}{a} \qquad \text{(EQN 15)}$$

where a is the radius of the leaflet cross-section, D is the diffusion coefficient for oxygen in water (0.002 $mm^2 \cdot sec^{-1}$ at 20 C) and b is the sum of the leaflet radius, a, and the boundary layer thickness. The surface area, S, for a leaflet section of length l is given by:

$$S = 2\pi \cdot a \cdot l \qquad \text{(EQN 16)}$$

Rearranging Equation 6,

$$\Delta C\ (mgO_2 \cdot mm^{-3}) = \frac{FLUX\ (mgO_2 \cdot sec^{-1}) \cdot R\ (sec \cdot mm^{-1})}{S\ (mm^2)} \qquad \text{(EQN 17)}$$

For *Myriophyllum spicatum* plants growing at PAR levels between 150 and 170 $\mu E \cdot m^{-2} \cdot sec^{-1}$, the leaflet radius averaged 0.2 mm. On the assumption that all photosynthesis occurred in leaflet tissues, the oxygen efflux for a leaflet section 1 mm long was approximately 8.4×10^{-9} $mgO_2 \cdot sec^{-1}$. Substituting for FLUX, a and l, and converting from mm^3 to liters,

$$\Delta C\ (mgO_2 \cdot l^{-1}) = 0.667 \cdot \ln(\frac{b}{0.2}) \qquad \text{(EQN 18)}$$

Values for b, the sum of leaflet radius, a, and boundary

layer thickness, can be specified to develop values for ΔC. Browse, *et al.*, (1979) and Smith and Walker (1980) pointed out that boundary thickness for macroscopic objects in water must be at least 10 μm in highly stirred systems and no more than 500 μm in "still" water. Equation 18 was plotted in Figure 13 for boundary thickness ranging from 0 to 1,000 μm. These results indicate that even if boundary layer thickness reached 1 mm, leaflets of *Myriophyllum spicatum* cannot develop oxygen partial pressures at the outer plant surface greater than 2 kPa above atmospheric saturation, when light levels are below 170 $\mu E \cdot m^{-2} \cdot sec^{-1}$.

Westlake (1978) found that shoots of *Myriophyllum spicatum* were light-saturated at 1,000 $\mu E \cdot m^{-2} \cdot sec^{-1}$; oxygen efflux at light saturation was 1.85 times greater than rates measured at 150-170 $\mu E \cdot m^{-2} \cdot sec^{-1}$ during this research. Substituting the light-saturated estimate for FLUX into Equation 17,

$$\Delta C \ (mgO_2 \cdot l^{-1}) = 1.23 \cdot \ln(\frac{b}{0.2}) \qquad \text{(EQN 19)}$$

Equation 19 was also plotted in Figure 13, showing ΔC values at the highest reported oxygen efflux for the species.

This exercise shows that even when oxygen efflux reaches light-saturated levels and there is minimal water movement, *Myriophyllum spicatum* leaflets cannot develop oxygen partial pressures at the exterior surface greater than 5 kPa above atmospheric saturation. As light levels (hence oxygen efflux) decrease, oxygen partial pressures at a plant's surface

Figure 13. Magnitude of the oxygen gradient outside leaflets of *Myriophyllum spicatum*, as a function of boundary layer thickness. A. Values calculated from Equation 18, using oxygen efflux values at 150 - 170 $\mu E \cdot m^{-2} \cdot sec^{-1}$ PAR. B. Values calculated from Equation 19 using estimated oxygen efflux at 1,000 $\mu E \cdot m^{-2} \cdot sec^{-1}$.

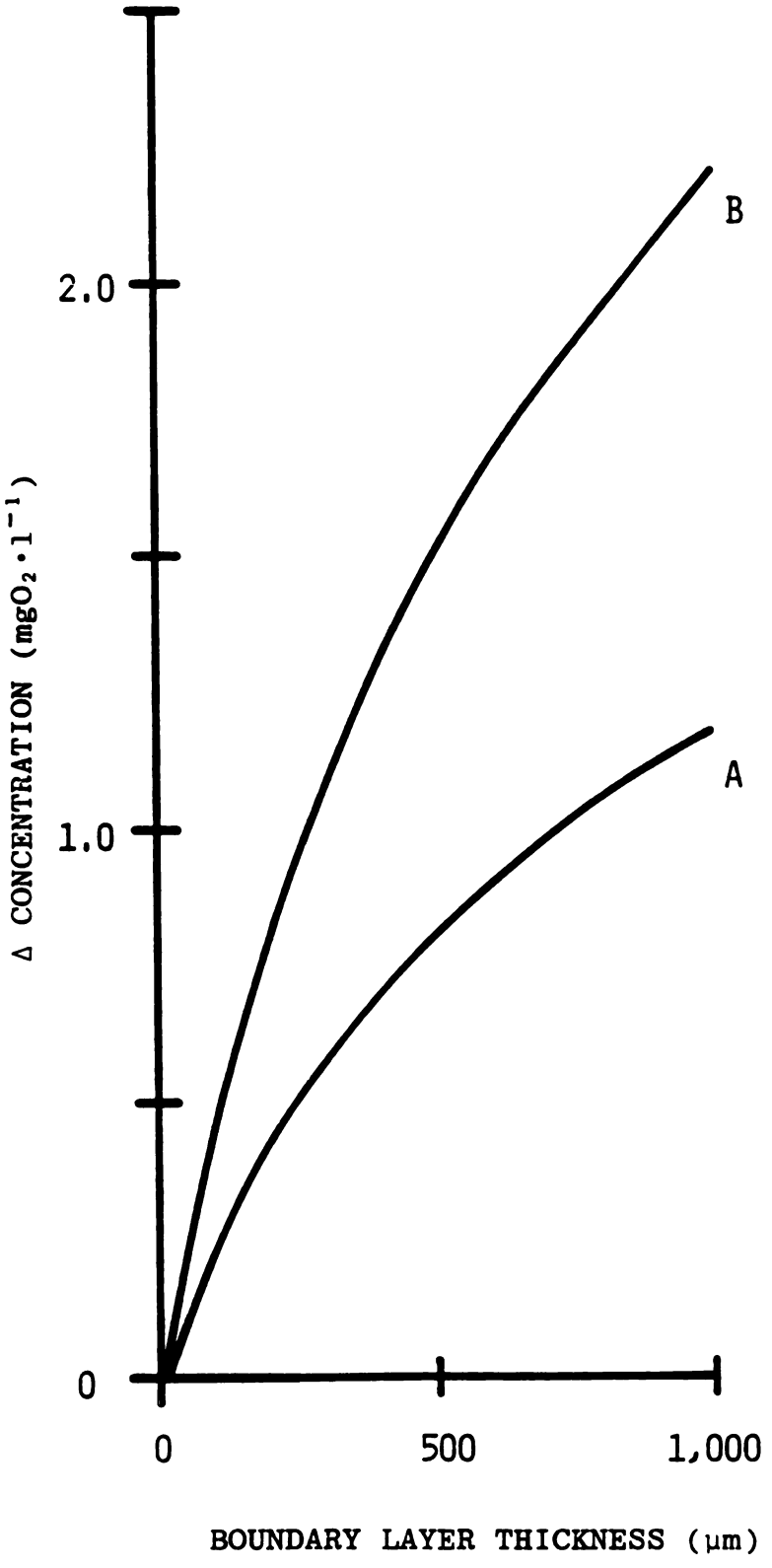
B
A
2.0
1.0
0
Δ CONCENTRATION ($mgO_2 \cdot l^{-1}$)
0
500
1,000
BOUNDARY LAYER THICKNESS (μm)

also decrease. The cylindrical shape of *Myriophyllum spicatum* leaflets allows rapid dispersion of photosynthetic oxygen production, minimizing back-pressure for lacunar oxygen accumulation. Like the stem lacunae, leaflet lacunae in this species must be formed and held open by cell structure.

The continuity of stem lacunae in *Myriophyllum spicatum*, shown in Figure A-4, provides the final evidence that gases in the internal atmosphere of these plants are stored at pressures less than the total pressures ($P_{atm} + P_h$) forcing inward against plants' exterior surfaces. A plant rooted at 4 m depth which reaches the water surface experiences 39 kPa hydrostatic pressure at its base and 0 kPa hydrostatic pressure at its apex. Since the stem lacunar system is continuous, gas pressures must be the same throughout. In a lacunar system held open entirely by gas pressurization, the apical region would be required to hold 39 kPa excess pressure. Alternatively, if the lacunar arch system held the gas spaces open, it would be required to hold against 39 kPa hydrostatic pressure just above the sediment surface. Partial excess gas pressurization resulting from photosynthetic oxygen production would lead to slight over-pressurization at the apex and reduced under-pressurization at the stem base. Oxygen diffusion considerations given above show that it is unlikely these plants can develop excess oxygen pressures as high as 39 kPa. Considering this, significant under-pressurization must occur in the basal portions of

stems greater than 2 m in length.

The strength of the lacunar arch system is lower in basal portions of long stems than in younger sections. The load-bearing character of the lacunar arch system is determined partly by the ratio of length to width for the septae. As length for a column increases relative to its width, its load-bearing ability decreases (Baumeister, 1958). This ratio increased from 1.0 in apical sections of *Myriophyllum spicatum* (Figure 9D) to 11.0 in sections taken 2 m below the shoot apex (Figure 12). Consequently, mature stem sections near the sediment surface appear more likely to collapse under hydrostatic pressure loads than younger, apical sections. This research and Dale's (1981) incorporated young, apical shoot sections of *Myriophyllum spicatum*, and both studies failed to link hydrostatic pressure to depth limits for this species in lakes.

Mature root sections (Figure A-5A) also had lacunar structures which were not suited to bear external crushing forces. These lysigenous lacunae had thin septae but lacked arch-like organization. Younger roots (A-5B) had small lacunae which may stand greater external pressures than mature sections, but expansion of these gas spaces by additional lysing weakens the strength of the cross-section. Dale (1981) found that root growth in *Myriophyllum spicatum* was significantly decreased at hydrostatic pressures greater than 135 kPa, yet he concluded that hydrostatic pressure probably had not limited depth distribution of this species

in lakes. Grace and Wetzel (1976) concluded that nutrient uptake from the root system in this species was an important aspect of its competitive ability. The depth limitation of *Myriophyllum spicatum* by the action of hydrostatic pressure on the plants' root system cannot be ruled out by existing data.

Evidence from field studies (Golubic, 1963; Frantz and Cordone, 1967; Spence, 1967; Sheldon and Boylen, 1977) pointed toward a disparity between depth distributions of lacunate and non-lacunate hydrophyte species. The principle hypothesis of this study held that hydrostatic pressure acted against the formation and function of lacunar spaces in the lacunate hydrophytes, restricting their depth distributions. The promotion of outward gas diffusion was proposed as the mechanism for lacunar disruption by hydrostatic pressure. The results of this research have shown that hydrostatic pressure did not promote outward gas diffusion because gases were stored at pressures which were independent of hydrostatic pressure. This was made possible by the lacunar arch system, which bore the load of hydrostatic pressure, avoiding the compression of lacunar gases within the range of pressures simulated. These results could not be generalized to mature plants in natural settings. The lacunar arch system in mature stem sections was weaker against external crushing forces than in apical shoot material used for this research. The root system may also be susceptible to crushing by hydrostatic pressure; data given by Dale (1981) support this contention.

LITERATURE CITED

LITERATURE CITED

American Public Health Association. 1975. Standard Methods for the Examination of Water and Wastewater. 14th ed. Washington, D.C., American Public Health Association. 1193 pp.

Arnon, D.I. 1949. Copper enzymes in isolated chloroplasts. Polyphenoloxidases in *Beta vulgaris*. Plant Physiol. 24:1-15.

Baumeister, T. 1958. Mark's Mechanical Engineers' Handbook. 6th ed. New York, McGraw-Hill. 2278 pp.

Bodkin, P.C., U. Posluszny, and H.M. Dale. 1980. Light and pressure in two freshwater lakes and their influence on the growth, morphology and depth limits of *Hippuris vulgaris*. Freshwater Biol. 10:545-552.

Bonner, J., and J.E. Varner. 1976. Plant Biochemistry. New York, Academic Press. 925 pp.

Browse, J.A., F.I. Dromgoole, and J.M.A. Brown. 1979. Photosynthesis in the aquatic macrophyte *Egeria densa*. III. Gas exchange studies. Aust. J. Plant Physiol. 6:499-512.

Campbell, G.S. 1977. An Introduction to Environmental Biophysics. New York, Springer-Verlag. 159 pp.

Crank, J. 1956. The Mathematics of Diffusion. Oxford, Clarendon Press. 341 pp.

Dale, H.M. 1957. Developmental studies of *Elodea canadensis* Michx. I. Morphological development at the shoot apex. Can. J. Bot. 35:13-24.

_____. 1981. Hydrostatic pressure as the controlling factor in the depth distribution of eurasian watermilfoil, *Myriophyllum spicatum* L. Hydrobiologia 79:239-244.

Fehrling, E. 1957. Die Wirkungen des Erhoten hydrostatischen Druckes auf Wachstum und Differenzierung submerser Blutenpflanzen. Planta 49:235-270.

Frantz, T.C., and A.J. Cordone. 1967. Observations on deep-water plants in Lake Tahoe, California and Nevada. Ecology, 48:709-714.

Gessner, F. 1952. Der Druck in seiner Bedeutung fur das Wachstum submerser Wasserpflanzen. Planta, 40:391-397.

Golubic, S. 1963. Hydrostatischer Druck, Licht, und submerse Vegetation im Vrana-See. Int. Rev. gesamten Hydrobiol. 48:1-7.

Grace, J.B., and R.G. Wetzel. 1976. The production biology of eurasian watermilfoil (*Myriophyllum spicatum* L.): a review. J. Aquat. Plant Manag. 16:1-11.

Hartman, R.T., and D.L. Brown. 1967. Changes in internal atmosphere of submerged vascular hydrophytes in relation to photosynthesis. Ecology, 48:252-258.

Hasman, M., and N. Inanc. 1957. Investigations on the anatomical structure of certain submerged, floating and amphibious hydrophytes. Istanb. Univ. Fen Fak. Mecm., ser. B, 22:137-153.

Hiscox, J.D., and G.F. Israelstam. 1979. A method for the extraction of chlorophyll from leaf tissue without maceration. Can. J. Bot., 57:1332-1334.

Hutchinson, G.E. 1957. A Treatise on Limnology. I. Geography, Physics, and Chemistry. New York, John Wiley and Sons. 1015 pp.

_____. 1975. A Treatise on Limnology. III. Limnological Botany. New York, John Wiley and Sons. 660 pp.

Lim, P.G. 1976. A field experiment with granular 2,4-D for control of eurasian watermilfoil, 1976. Studies on aquatic macrophytes, Pt. 10. British Columbia, Water Investigations Branch, Report No. 2613. 105 pp.

Payne, F.C. 1977. Floristics of Harding Lake, Alaska. M.S. Thesis. Michigan State University. 99 pp.

Pearsall, W.H. 1920. The aquatic vegetation of the English Lakes. J. Ecol., 8:163-199.

Pond, R.H. 1905. The relation of aquatic plants to the substratum. Rep. U.S. Fish. Comm., 21:483-526.

Salisbury, F.B., and C.W. Ross. 1978. Plant Physiology. Belmont, California, Wadsworth Pub. Co. 436 pp.

Sass, J.E. 1951. Botanical Microtechnique. Ames, Iowa, The Iowa State Univ. Press. 228.

Sculthorpe, C.D. 1967. The Biology of Aquatic Vascular Plants. London, Edward Arnold, Ltd. 610 pp.

Sheldon, R.B. and C.W. Boylen. 1977. Maximum depth inhabited by aquatic vascular plants. Amer. Midl. Nat., 97:248-254.

Smith, F.A., and N.A. Walker. 1980. Photosynthesis by aquatic plants: effects of unstirred layers in relation to assimilation of CO_2 and HCO_3^- and to carbon isotopic discrimination. New Phytol. 86:245-259.

Spence, D.H.N. 1967. Factors controlling the distribution of freshwater macrophytes with particular reference to the lochs of Scotland. J. Ecol., 55:147-170.

Spence, D.H.N. and J. Chrystal. 1970a. Photosynthesis and zonation of freshwater macrophytes. I. Depth distributions and shade tolerance. New Phytol., 69:205-215.

_____. 1970b. Photosynthesis and zonation of freshwater macrophytes. II. Adaptability of species of deep and shallow waters. New Phytol., 69:217-227.

Stross, R.G. 1979. Density and boundary regulations of the *Nitella* meadow in Lake George, New York. Aquat. Bot., 6:285-300.

Vidaver, W. 1972. Effects of pressure on the metabolic processes of plants. *In:* M.A. Sleigh and A.G. MacDonald, eds., The effects of pressure on organisms. Proc. Symp. Soc. Exp. Biol., 26:159-174.

Westlake, D.F. 1978. Rapid exchange of oxygen between plant and water. Verh. Int. Ver. Limnol., 20:2363-2367.

Wilson, L.R. 1935. Lake development and plant succession in Vilas County, Wisconsin. Pt. I. The medium hard water lakes. Ecol. Monogr., 5:207-247.

_____. 1937. A quantitative and ecological study of the larger aquatic plants of Sweeny Lake, Oneida County, Wisconsin. Bull. Torrey Bot. Club, 64:199-208.

_____. 1941. The larger aquatic vegetation of Trout Lake, Vilas County, Wisconsin. Trans. Wisconsin Acad. Sci., Arts, Lett., 33:135-146.

APPENDICES

APPENDIX I

SPECTRAL COMPOSITION OF HIGH INTENSITY DISCHARGE SODIUM LAMPS AND FOUR NATURAL LIGHT ENVIRONMENTS

Figure A1. Spectral characterization of photosynthetically active radiation (PAR) for four sources: 1. Clear-sky terrestrial solar curve at East Lansing, Michigan, at noon on the summer solstice (▽); 2. Lake George, New York, at 10 m depth under clear sky (⬡); 3. Lake Michigan off Grand Haven at 10 m depth under high overcast (□); 4. Lawrence Lake, Barry County, Michigan, at 10 m depth during July, under clear sky (○). Each curve is adjusted to a total PAR of 1,000 $\mu E \cdot m^{-2} \cdot sec^{-1}$ for comparison.

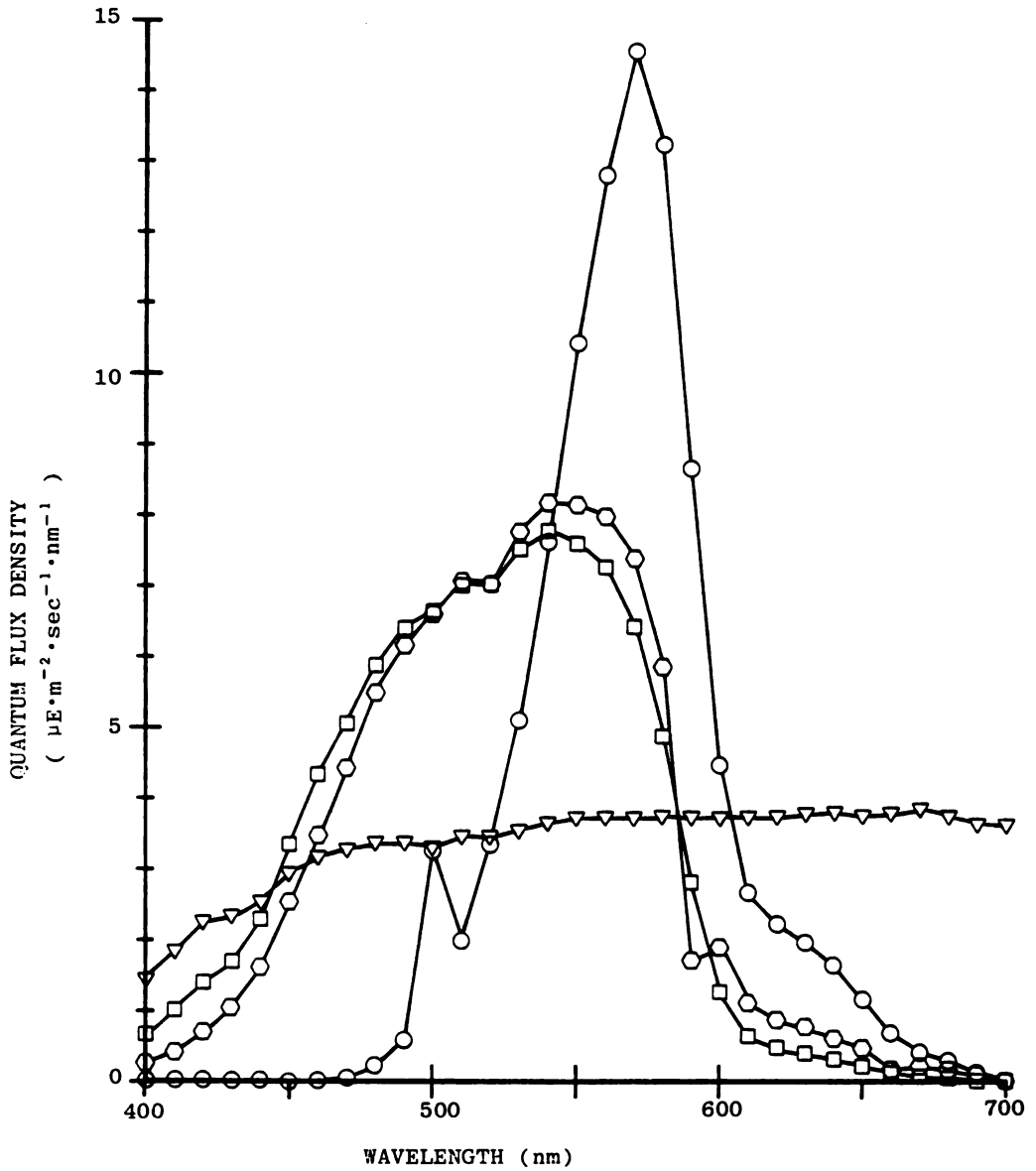
15
10
5
0
400
500
600
700
QUANTUM FLUX DENSITY
(μE·m⁻²·sec⁻¹·nm⁻¹)
WAVELENGTH (nm)

Figure A2. Spectral characterization of photosynthetically active radiation (PAR) emitted by high intensity discharge (HID) sodium lamps. The curve is adjusted for total PAR of 1,000 $\mu E \cdot m^{-2} \cdot sec^{-1}$.

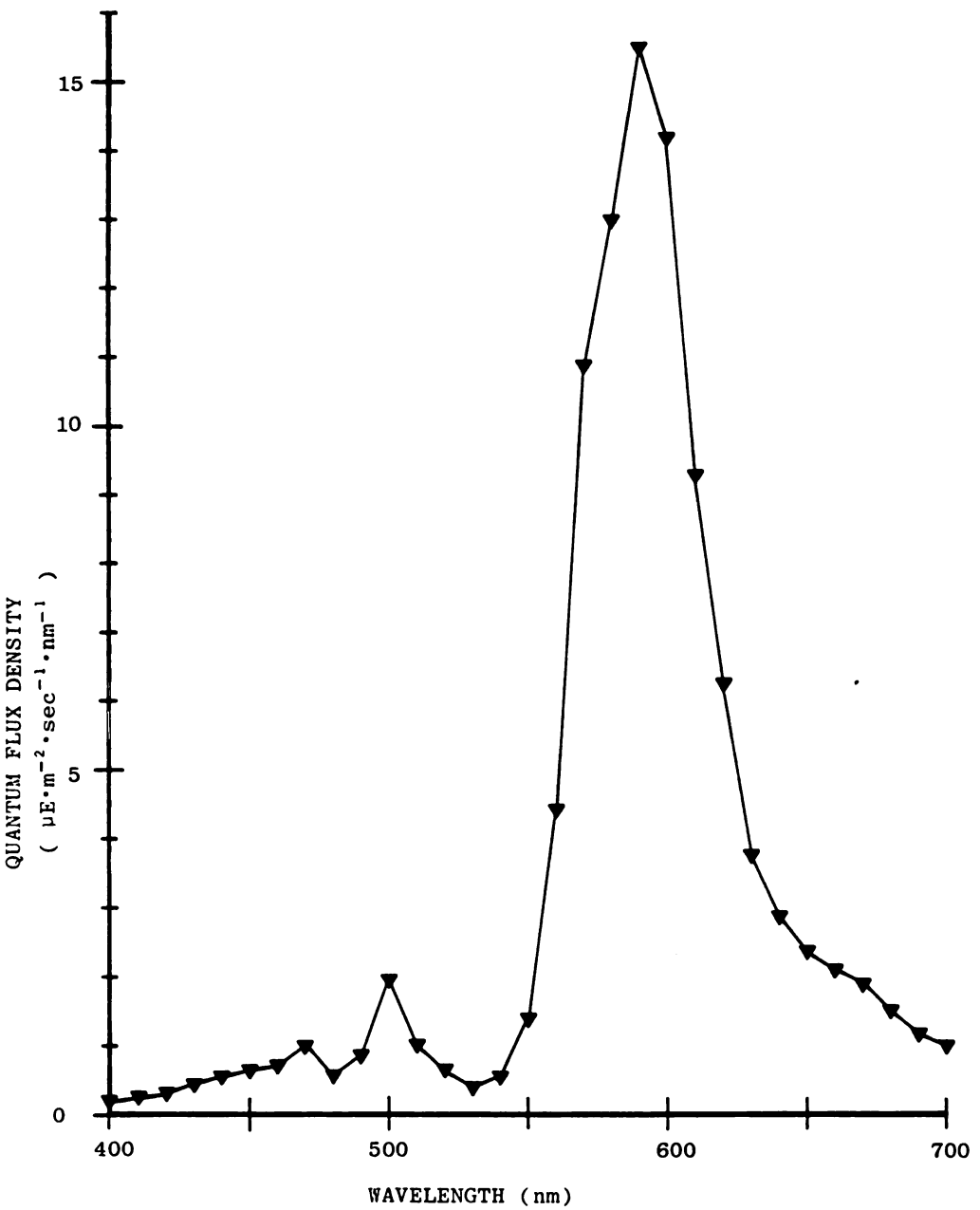
15
10
5
0
400
500
600
700
QUANTUM FLUX DENSITY
(μE·m⁻²·sec⁻¹·nm⁻¹)
WAVELENGTH (nm)

APPENDIX II

RESULTS OF PRELIMINARY EXPERIMENTS ON THE INFLUENCE OF EXTERNAL OXYGEN CONCENTRATION ON LACUNAR OXYGEN STORAGE IN *MYRIOPHYLLUM SPICATUM*.

Table A1. Results of preliminary experiments on the influence of external oxygen concentration on lacunar oxygen storage. Experiment 1: all chambers were closed for oxygen accumulation during the final three hours of the light period, then were flushed to ambient oxygen level.

	NET OXYGEN INFLUX $mgO_2 \cdot h^{-1} \cdot g^{-1}DW$		
CHAMBER	HOUR 1	HOUR 2	HOUR 12
1	0.273	0.545	0.455
2	0.200	0.400	0.440
3	0.232	0.588	0.510
4	0.000	0.434	0.528
5	0.310	0.310	0.000
6	+0.276†	0.423	0.331
7	0.000	0.527	0.344
8	0.000	0.483	0.420

†Positive influx value indicates oxygen was released during the first hour of darkness.

Table A2. Results of preliminary experiments on the influence of external oxygen concentration on lacunar oxygen storage. Experiment 2: chambers 2, 3, 6 and 7 were closed for the final 8 hours of the light period, then were flushed to ambient oxygen concentration. The remaining 4 chambers flowed at 150 $ml \cdot min^{-1}$ throughout the light period.

	NET OXYGEN INFLUX $mgO_2 \cdot h^{-1} \cdot g^{-1}DW$	
CHAMBER	HOUR 1	HOUR 2
1	0.364	0.636
2	+0.267†	0.200
3	+0.232†	0.387
4	0.283	0.660
5	0.517	0.000
6	+0.092†	0.276
7	0.229	0.573
8	0.839	1.049

†Positive influx value indicates oxygen was released during the first hour of darkness.

Table A3. Results of preliminary experiments on the influence of external oxygen concentration on lacunar oxygen storage. Experiment 3: Chambers 2, 3, 6 and 7 were closed for the final 8 hours of the light period, then were flushed to ambient oxygen concentration. Chambers 1, 4 and 8 flowed at 150 $ml \cdot min^{-1}$ throughout the light period; chamber 5 flowed at ≈ 5 $ml \cdot min^{-1}$ throughout the light period.

	NET OXYGEN INFLUX $mgO_2 \cdot h^{-1} \cdot g^{-1}DW$		
CHAMBER	HOUR 1	HOUR 2	HOUR 3
1	0.545	0.727	0.727
2	0.000	0.533	0.400
3	0.000	0.464	0.619
4	0.943	0.943	0.943
5	0.414	0.207	0.000
6	0.000	0.368	0.368
7	0.458	0.229	0.229
8	1.049	1.049	1.049

APPENDIX III

RESULTS OF EXPERIMENTS ON THE INFLUENCES OF HYDROSTATIC PRESSURE AND LIGHT ON NET OXYGEN EFFLUX AND LACUNAR OXYGEN STORAGE IN *MYRIOPHYLLUM SPICATUM*.

Table A4. Results of experiments on the influence of light and hydrostatic pressure on net oxygen efflux (apparent photosynthesis) in *Myriophyllum spicatum*. Values for PAR are given as $\mu E \cdot m^{-2} \cdot sec^{-1}$; values for net oxygen efflux (NOE) are given as $mgO_2 \cdot h^{-1} \cdot mg^{-1}$Chl-*a*. The pressure level for each experiment is given in kPa above atmospheric pressure.

	I-A (10 kPa)		I-B (67 kPa)		I-C (67 kPa)		I-D (101 kPa)		I-E (152 kPa)	
PLANT	PAR	NOE	PAR	NOE	PAR	NOE	PAR	NOE	PAR	NOE
I-1	104	0.89	174	1.88	68	0.87	174	1.41	68	0.87
I-2	104	0.81	145	1.59	60	0.73	145	1.22	60	0.79
I-3	104	1.02	174	1.83	68	0.76	174	1.29	68	0.91
I-4	104	0.75	137	1.58	57	0.68	134	1.20	57	0.83
I-5	104	0.79	132	1.42	55	0.55	132	1.11	55	0.63
I-6	104	0.83	115	1.36	48	0.41	115	1.09	48	0.41
I-7	104	0.92	132	1.45	52	0.48	132	lost	52	0.69
I-8	104	0.88	117	1.40	47	0.49	117	1.15	47	0.61

Table A4, continued.

	II-A (10 kPa)		II-B (67 kPa)		II-C (67 kPa)		II-D (67 kPa)		II-E (67 kPa)	
PLANT	PAR	NOE	PAR	NOE	PAR	NOE	PAR	NOE	PAR	NOE
II-1	104	1.24	162	1.91	69	0.92	27	0.38	27	0.26
II-2	104	1.55	130	1.97	53	0.85	22	0.28	22	0.24
II-3	104	1.71	161	1.52	67	0.95	29	0.19	29	0.16
II-4	104	1.00	129	1.50	54	0.67	23	0.25	23	0.14
II-5	104	1.30	160	1.67	63	0.76	26	0.21	26	0.17
II-6	104	1.36	144	1.63	59	0.51	24	0.11	24	0.09
II-7	104	1.43	160	1.91	66	0.92	25	0.32	25	0.29
II-8	104	1.51	147	1.81	59	0.74	24	0.20	24	0.17

Table A4, continued.

	III-A (10 kPa)		III-B (152 kPa)		III-C (152 kPa)		III-D (152 kPa)	
PLANT	PAR	NOE	PAR	NOE	PAR	NOE	PAR	NOE
III-1	- - - - - - - - - - - - - lost - - - - - - - - - - - - -							
III-2	104	1.39	130	1.67	53	0.79	22	0.16
III-3	104	1.58	161	1.78	67	0.94	29	0.25
III-4	104	1.29	129	1.70	54	0.88	23	0.09
III-5	104	1.66	160	1.66	63	0.75	26	0.04
III-6	104	1.69	144	1.57	59	0.72	24	0.12
III-7	104	1.15	160	1.45	66	0.66	25	0.12
III-8	104	1.28	147	1.78	59	0.69	24	0.05

Table A4, continued.

	IV-A (10 kPa)		IV-B (101 kPa)		IV-C (101 kPa)		IV-D (101 kPa)		IV-E (101 kPa)	
PLANT	PAR	NOE	PAR	NOE	PAR	NOE	PAR	NOE	PAR	NOE
IV-1	104	1.07	162	1.01	69	0.57	69	0.50	27	0.06
IV-2	104	1.02	130	1.02	53	0.39	53	0.39	22	0.00
IV-3	104	1.53	161	1.35	67	0.45	67	0.63	29	0.09
IV-4	104	1.18	129	1.07	54	0.54	54	0.48	23	0.03
IV-5	104	1.03	160	1.13	63	0.46	63	0.43	26	0.07
IV-6	104	1.51	144	1.21	59	0.60	59	0.50	24	0.08
IV-7	104	1.72	160	1.77	66	0.75	66	0.70	25	0.14
IV-8	104	1.63	147	1.27	59	0.51	59	0.41	24	0.00

Table A5. Fresh weight (FW), total chlorophyll (Chl-t) and chlorophyll-*a* (Chl-*a*) for shoots included in experiments on the influences of hydrostatic pressure and light on net photosynthesis in *Myriophyllum spicatum*.

PLANT	Chl-*a* (mg)	Chl-t (mg)	FW (g)	RATIO Chl-*a*/Chl-t ($mg \cdot mg^{-1}$)	RATIO Chl-t/FW ($mg \cdot g^{-1}$)
I-1	0.224	0.314	0.815	0.71	0.39
I-2	0.246	0.341	0.584	0.72	0.58
I-3	0.197	0.277	0.596	0.71	0.47
I-4	0.200	0.282	0.526	0.71	0.54
I-5	0.190	0.266	0.540	0.72	0.49
I-6	0.221	0.307	0.581	0.72	0.53
I-7	0.218	0.305	0.573	0.72	0.53
I-8	0.247	0.345	0.827	0.72	0.42
II-1	0.315	0.430	0.600	0.73	0.72
II-2	0.213	0.296	0.499	0.72	0.59
II-3	0.316	0.434	0.773	0.73	0.56
II-4	0.359	0.486	0.463	0.74	1.05
II-5	0.288	0.383	0.399	0.75	0.96
II-6	0.276	0.371	0.428	0.74	0.87
II-7	0.283	0.377	0.494	0.75	0.76
II-8	0.299	0.400	0.511	0.75	0.78

Table A5, continued.

PLANT	Chl-*a* (mg)	Chl-t (mg)	FW (g)	RATIO Chl-*a*/Chl-t ($mg \cdot mg^{-1}$)	RATIO Chl-t/FW ($mg \cdot g^{-1}$)
III-1	- - - - - - - - - - - - - - -		lost	- - - - - - - - - - - - - - - - - - -	
III-2	0.324	0.432	0.799	0.75	0.54
III-3	0.304	0.403	0.708	0.76	0.57
III-4	0.256	0.343	0.524	0.75	0.66
III-5	0.199	0.266	0.528	0.75	0.50
III-6	0.249	0.336	0.764	0.74	0.44
III-7	0.249	0.333	0.646	0.75	0.52
III-8	0.152	0.208	0.594	0.73	0.35
IV-1	0.238	0.318	0.914	0.75	0.35
IV-2	0.192	0.259	0.520	0.74	0.50
IV-3	0.167	0.224	0.515	0.75	0.44
IV-4	0.280	0.374	0.953	0.75	0.39
IV-5	0.424	0.564	0.977	0.75	0.58
IV-6	0.298	0.398	0.877	0.75	0.45
IV-7	0.279	0.371	0.843	0.75	0.44
IV-8	0.295	0.393	0.890	0.75	0.44

Table A6. Results of experiments on the influence of ambient oxygen concentration on lacunar oxygen storage at 67 kPa above atmospheric pressure. Ambient oxygen concentration (O_{2_a}) is given in $mgO_2 \cdot l^{-1}$; hourly respiration rates (R_n) are given in $mgO_2 \cdot h^{-1} \cdot l^{-1}$ measured in 300 ml sample volume. Lacunar storage values (LS) were calculated according to Equation 8.

PLANT	O_{2_a}	R_1	R_2	R_3	R_4	R_5	R_6	R_7	R_8	$\overline{R}_{2-6}$	LS
1	31.7	0.10	0.48	0.45	0.48	0.45	0.48	0.40	0.35	0.468	0.98
2	8.1	0.35	0.43	0.40	0.33	0.45	0.33	0.35	0.40	0.388	0.10
3	24.4	0.00	0.28	0.40	0.33	0.40	0.28	0.35	0.35	0.338	1.00
4	17.5	0.15	0.38	0.40	0.33	0.35	0.33	0.50	0.30	0.358	0.58
5	8.1	0.15	0.38	0.30	0.38	0.30	0.33	0.30	0.25	0.338	0.56
6	12.8	0.15	0.38	0.25	0.18	0.25	0.23	0.15	0.15	0.258	0.42
7	11.4	0.15	0.23	0.35	0.28	0.45	0.33	0.30	0.30	0.328	0.54
8	25.0	0.05	0.18	0.15	0.28	0.35	0.33	0.25	0.30	0.258	0.81

Table A7. Results of experiments on the influence of ambient oxygen concentration on lacunar oxygen storage at 152 kPa above atmospheric pressure. Ambient oxygen concentration (O_{2_a}) is given in $mgO_2 \cdot l^{-1}$; hourly respiration rates (R_n) are given in $mgO_2 \cdot h^{-1} \cdot l^{-1}$measured in 300 ml sample volumes. Lacunar storage values (LS) were calculated according to equation 8.

PLANT	O_{2_a}	R_1	R_2	R_3	R_4	R_5	R_6	R_7	R_8	$\overline{R}_{2-6}$	LS
1	20.4	0.10	0.20	0.28	0.30	0.38	0.35	0.33	0.15	0.30	0.67
2	8.5	0.10	0.25	0.18	0.20	0.13	0.20	0.18	0.05	0.19	0.47
3	13.7	0.15	0.25	0.28	0.35	0.48	0.35	0.28	0.05	0.34	0.56
4	10.8	0.45	0.40	0.38	0.40	0.33	0.35	0.33	0.25	0.37	-0.22
5	8.7	0.00	0.10	0.08	0.15	0.08	0.35	0.03	0.00	0.15	1.00
6	10.3	0.20	0.45	0.13	0.35	0.23	0.05	0.23	0.10	0.24	0.17
7	8.1	0.35	0.40	0.48	0.40	0.28	0.15	0.23	0.15	0.34	-0.03
8	13.3	0.10	0.30	0.13	0.45	0.28	0.20	0.13	0.05	0.27	0.63

Table A8. Estimates of fresh weight (FW) and dry weight (DW) for shoots involved in lacunar storage experiments at 67 kPa above atmospheric pressure.

PLANT	FW (g)	DW (g)
1	0.697	0.184
2	0.501	0.113
3	0.621	0.148
4	0.491	0.096
5	0.502	0.091
6	0.517	0.099
7	0.555	0.104
8	0.560	0.129

Table A9. Results of experiments on the influence of ambient oxygen concentration on lacunar oxygen storage at 67 kPa above atmospheric pressure. Ambient oxygen concentration (O_{2_a}) is given in $mgO_2 \cdot l^{-1}$; hourly respiration rates (R_n) are given in $mgO_2 \cdot h^{-1} \cdot g^{-1}DW$. Lacunar storage values (LS) were calculated according to Equation 8.

PLANT	O_{2_a}	R_1	R_2	R_3	R_4	R_5	R_6	R_7	R_8	$\bar{R}_{2-6}$	LS
1	31.7	0.16	0.77	0.73	0.77	0.73	0.77	0.65	0.57	0.76	0.98
2	8.1	0.93	1.13	1.06	0.86	1.20	0.86	0.93	1.06	1.02	0.10
3	24.4	0.00	0.56	0.81	0.66	0.81	0.56	0.71	0.71	0.68	1.00
4	17.5	0.47	1.17	1.25	1.02	1.09	1.02	1.56	0.94	1.11	0.58
5	8.1	0.50	1.24	0.99	1.24	0.99	1.07	0.99	0.82	1.10	0.56
6	12.8	0.46	1.14	0.76	0.53	0.76	0.68	0.46	0.46	0.82	0.42
7	11.4	0.43	0.65	1.01	0.79	1.30	0.94	0.87	0.87	0.94	0.54
8	25.0	0.12	0.41	0.35	0.64	0.81	0.76	0.58	0.70	0.59	0.81

Table A10. Results of measurements of net oxygen efflux following lacunar oxygen storage trials for plants at 67 kPa above atmospheric pressure. Hourly net photosynthesis values (P_n) are reported in $mgO_2 \cdot h^{-1} g^{-1} DW$. Photosynthetically active irradiance values (PAR) are reported in $\mu E \cdot m^{-2} \cdot sec^{-1}$ for each plant. Results were calculated from one 300 ml sample collected at hourly intervals. No flushing was allowed between sample collections.

PLANT	PAR	P_1	P_2	P_3	P_4	P_5	P_6	P_7	P_8	P_9	P_{10}
1	162	0.93	3.05	2.77	2.77	3.13	2.77	2.97	2.85	3.05	2.56
2	130	1.78	4.17	4.51	3.72	4.17	4.25	3.90	3.72	4.04	3.11
3	161	1.56	3.39	3.45	3.45	3.49	3.14	3.39	3.55	3.59	2.98
4	129	1.94	4.59	4.84	4.84	5.22	4.84	4.75	4.84	4.91	4.59
5	160	1.88	4.19	3.96	3.96	4.52	4.12	3.53	4.29	5.01	3.53
6	144	1.88	4.00	3.48	3.79	4.15	3.33	3.24	3.94	3.85	2.94
7	160	1.79	4.24	4.47	4.62	4.24	4.04	3.95	4.04	4.53	3.66
8	147	1.67	3.42	3.49	3.49	3.65	3.60	3.30	3.26	3.30	2.60

Table A10, continued.

PLANT	P_{11}	P_{12}	P_{13}	P_{14}	P_{15}
1	2.89	2.23	2.64	2.48	1.96
2	4.83	3.24	3.37	3.24	2.79
3	3.89	0.04	2.98	2.98	2.53
4	5.84	4.28	4.75	4.59	3.91
5	5.51	3.86	4.19	4.19	3.46
6	4.76	3.39	3.24	3.39	2.58
7	5.25	4.53	4.10	4.10	3.17
8	3.53	2.95	2.84	3.07	2.44

APPENDIX IV

RESULTS OF ANATOMICAL STUDIES OF *MYRIOPHYLLUM SPICATUM*.

Figure A3. Typical leaf structure in *Myriophyllum spicatum*.
A. Transverse cross-section through rachis; lacunae are seen as clear areas in the mesophyll.
B. Transverse cross-section through leaflet; lacunae are seen as small gaps between mesophyll cells.

A

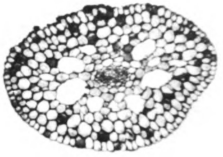

0.5 mm

B

0.5 mm

Figure A4. Typical configuration of a node in the stem of *Myriophyllum spicatum*, demonstrating the maximum constriction of the stem lacunar system. A. Transverse cross-section through node showing leaf traces; notice that rachis lacunae are also visible, but do not join stem lacunae. Leaf traces decrease lacunar cross-section by 40%. B. Transverse cross-section above node at the point where adventitious roots exit the stem. Lacunar cross-sectional area is reduced 60-70% in this section. No lacunae are visible in the root. C. Longitudinal cross-section through node, showing leaf traces crossing through lacunae.

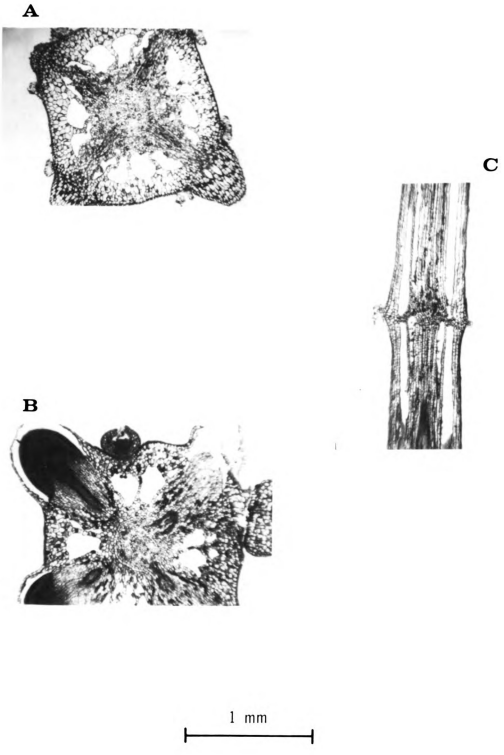
A
B
C
1 mm

Figure A5. Transverse cross-sections through *Myriophyllum spicatum* roots. A. Mature primary root, showing large, lysigenous lacunar spaces. Notice that the lacunar arch structure visible in stem sections and, to a lesser extent in the rachis secitons, is not apparent in the roots. B. Young primary root, showing small lacunae (seen as gaps between cortical cells).

A

0.5 mm

B

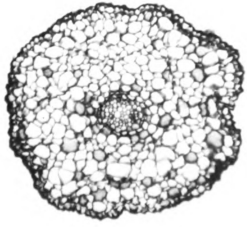

0.25 mm

Figure A-6. View into the stem lacunae of *Myriophyllum spicatum* under scanning electron microscope (SEM). Septum walls consist of sandbag-shaped cells, organized into the lacunar arch system. Many drusae are seen attached to the septae.

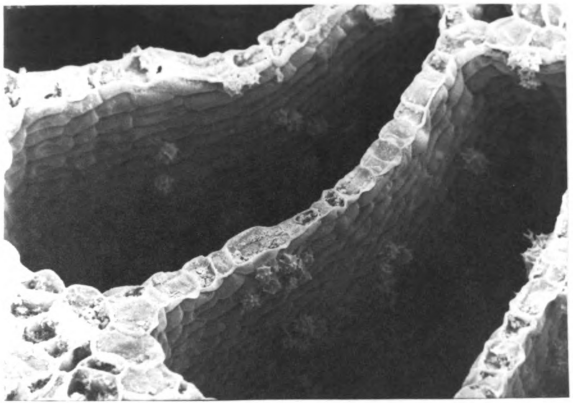

0.2 mm

Figure A7. View of druse attached to the septum wall of a stem lacuna in mature stem of *Myriophyllum spicatum*. Photograph made under SEM.

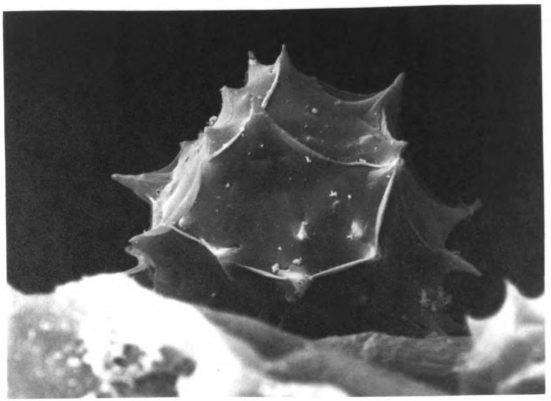

20 µm

Figure A8. Interior view of druse in *Myriophyllum spicatum* stem, showing crystal structure and the cell wall which encloses them. Notice that the druse wall is continous with the walls of the septum cells, arising from the junction of two septum cells.

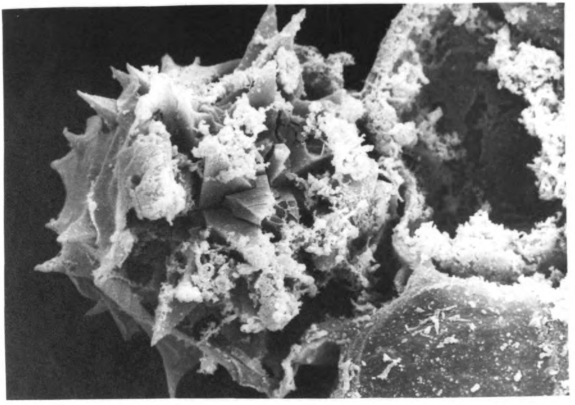

20 µm

MICHIGAN STATE UNIV. LIBRARIES
31293104292390